The Nuclear and Circum-nuclear Stellar Population in Seyfert 2 Galaxies: Implications for the Starburst-AGN Connection

Rosa M. González Delgado
Instituto de Astrofísica de Andalucía (CSIC), Apdo. 3004, 18080 Granada, Spain
Electronic mail: rosa@iaa.es

Timothy Heckman
Department of Physics & Astronomy, JHU, Baltimore, MD 21218
Adjunct Astronomer at STScI
Electronic mail: heckman@pha.jhu.edu

and

Claus Leitherer
Space Telescope Science Institute, 3700 San Martin Drive, Baltimore, MD 21218
Electronic mail: leitherer@stsci.edu

Received ________________________; accepted ________________________

To be published in The ΣAstrophysical Journal, 2001, 546, Jan 10 issue

ABSTRACT

We report the results of a spectroscopic investigation of a sample of 20 of the brightest type 2 Seyfert nuclei. Our goal is to search for the direct spectroscopic signature of massive stars, and thereby probe the role of circumnuclear starbursts in the Seyfert phenomenon. The method used is based on the detection of the higher order Balmer lines and HeI lines in absorption and the Wolf-Rayet feature at ∼4680 Å in emission. These lines are strong indicators of the presence of young (a few Myrs) and intermediate-age (a few 100 Myrs) stellar populations. In over half the sample, we have detected HeI and/or strong stellar absorption features in the high-order (near-UV) Balmer series together with relatively weak lines from an old stellar population. In three others we detect a broad emission feature near 4680 Å that is most plausibly ascribed to a population of Wolf-Rayet stars (the evolved descendants of the most massive stars). We therefore conclude that the blue and near-UV light of over half of the sample is dominated by young and/or intermediate age stars. The "young" Seyfert 2's have have larger far-IR luminosities, cooler mid/far-IR colors, and smaller [OIII]/Hβ flux ratios than the "old" ones. These differences are consistent with a starburst playing a significant energetic role in the former class. We consider the possibility that there may be two distinct sub-classes of Seyfert 2 nuclei ("starbursts" and "hidden BLR"). However, the fact that hidden BLRs have been found in three of the "young" nuclei argues against this, and suggests that nuclear starbursts may be a more general part of the Seyfert phenomenon.

Subject headings: galaxies: active – galaxies: nuclei – galaxies: Seyfert – galaxies: starburst – galaxies: stellar content

1. Introduction

According to the standard unified scheme for radio-quiet AGN, Seyfert 2 (S2) galaxies contain a Seyfert 1 (S1) nucleus that is obscured by a circum-nuclear torus of dust and gas. However, electrons and/or dust grains located along the polar axis of the torus can reflect the light from the hidden nucleus, allowing it to be seen in polarized light. Generally speaking the optical continuum of S2 nuclei can be classified into two components: a red continuum which is very similar to that of elliptical galaxies or early-type galactic bulges, and a bluer continuum in which the stellar lines are inconspicuous (the 'featureless continuum', or FC). According to the unified picture, the FC was believed to be scattered light from the hidden S1 nucleus. It dominates the ultraviolet continuum and contributes between 10% and 50% to the optical light.

However, this interpretation is not completely correct because after the contribution of the old stars is removed, the remaining optical continuum has a significantly lower fractional polarization than the broad optical emission lines (Tran 1995a,b,c). Therefore another unpolarized component has to contribute to the FC. Tran (1995c) suggests that the unpolarized component is optically thin thermal emission from warm gas, that is heated by the central hidden source. In contrast, Cid-Fernandes & Terlevich (1995) and Heckman et al. (1995) suggest that the unpolarized component is a young but dust-reddened stellar population, possibly associated with the obscuring torus.

Evidence that the unpolarized FC component in S2 nuclei is associated with young massive stars has been found in the last two years. In fact, to investigate the origin of the FC in S2 galaxies and the possible connection between the starburst and Seyfert phenomenon, we started a program to study the ultraviolet (UV) continuum emitted by their nuclei with the goal of detecting stellar features from massive stars. We choose this spectral range because it is the most favorable wavelength range to detect massive stars, since these stars emit most of their flux at UV and far-UV wavelengths. In contrast, older stars contribute significantly at optical and longer wavelengths. Therefore, UV images provide potentially direct information about the location of recent unobscured star forming regions. UV images of starburst galaxies show that a significant fraction of the massive stars are formed in very compact stellar clusters (Meurer et al. 1995) that have sizes of a few pc. Therefore, the morphology of the UV light in S2 nuclei can indicate whether these nuclei harbor a starburst. However, conclusive evidence for the presence of a starburst in the nuclei of S2 galaxies can be obtained from their UV spectrum. The UV spectrum of a starburst is very rich in absorption lines due both to stars and interstellar gas. The strongest stellar lines are formed in the wind of massive stars. These lines are blueshifted by 2000-3000 km s^{-1} and/or show a P-Cygni profile. Stellar photospheric lines are also present, but these features are much weaker than the wind resonance lines and are not shifted in velocity. Strong resonance absorption lines also form in the interstellar gas. These lines are often blueshifted by several hundred km s^{-1} (González Delgado et al. 1998a). However, these interstellar lines cannot be taken as a proof of the existence of a starburst, because a non-stellar Σcentral engine can also drive a similar kind of outflow. Conclusive proof that the UV emission in the S2 nuclei comes from a starburst is obtained if stellar wind resonance lines (such as NV λ1240, SiIV λ1400 and CIV λ1550) are detected in their spectra.

These stellar wind resonance lines were detected with Hubble Space Telescope's (HST) Goddard High Resolution Spectrometer (GHRS) in four (Mrk 477, NGC 7130, NGC 5135 and IC 3639) of the brightest UV S2 nuclei of our sample (see section 2). The data indicate that the UV light is dominated by the starburst component (Heckman et al. 1997, González Delgado et al. 1998b; hereafter H97 and GD98, respectively), with the contribution of the hidden nucleus amounting to less than 20% of the total emission. Comparing the strength of the wind lines with those predicted by evolutionary synthesis models (Leitherer et al. 1995), we conclude that in these S2 nuclei, the starbursts are of short duration, with ages between 4 and 6 Myr. We find that, after correcting the observed UV continuum for dust extinction using the starburst attenuation law (Calzetti, Kinney, & Storchi-Bergmann, 1994), the bolometric luminosity of these starbursts ($\sim 10^{10}$ L$\odot$) is similar to the estimated luminosity of the hidden S1 nucleus. Signatures of massive stars have been found also in other active galactic nuclei (AGN). Maoz et al. (1998) detect stellar features from massive stars in three of the seven brightest UV LINERs observed with HST. These nuclei seem to belong to the LINER sub-class that Heckman (1996) and Filippenko & Terlevich (1992) have proposed may be metal-rich starbursts. In these objects the estimated bolometric luminosity of the starbursts ranges between $\sim 10^8$ to 10^9 L$\odot$. This is significantly lower than that in S2 nuclei, but is similar to the luminosities of super-star clusters that are believed to be the building blocks of starburst galaxies. Therefore, we conclude from this previous work that, at least in the UV- brightest S2 and LINERs, the light is often dominated by a starburst. Hot young stars are the origin of the unpolarized FC component in at least some S2 nuclei.

Additional evidence for the presence of massive stars has been found in the optical spectra of a few Seyfert galaxies. At 4680 Å the spectra of these Seyfert nuclei show a broad emission feature (H97; Storchi-Bergmann, Cid Fernandes & Schmitt 1998 (S98); Tran et al. 1999; Kunth & Contini 1999). The origin of this broad emission cannot be due to scattered light from the hidden S1 nucleus, because their polarized spectra do not show this feature. Alternatively, it has been proposed that this emission has a stellar origin, produced by Wolf-Rayet stars, the descendants of massive stars. However, there is no additional evidence for the presence of a starburst in the nuclei of these Seyferts, except in Mrk 477. In this S2 nucleus, the detection of ultraviolet resonance lines formed in the wind of massive stars strongly supports the interpretation that the broad emission at 4680 Å is produced by Wolf-Rayet stars (H97).

Another approach to study the origin of the FC has been carried out by Cid Fernandes and collaborators (Cid Fernandes, Storchi-Bergmann & Schmitt 1998, hereafter CF98). They have measured the optical continuum flux in selected windows and the equivalent widths of several optical stellar absorption lines (mainly CaII K and H, the G band, MgI+MgH feature and the NaI D doublet) as a function of the distance from the nucleus for a sample of Seyfert galaxies. The main result obtained is that the stellar lines toward the nucleus are not significantly diluted, suggesting that if a FC is present, it contributes less than 10% to the optical light. The exception to this behaviour is found in objects that harbor a nuclear starburst. In these cases, the equivalent widths of the stellar lines are strongly diluted. Spectral synthesis using the stellar lines listed above indicate that the Seyfert 2 nuclei of their sample have a larger contribution from stars with ages of 100 Myr (Schmitt, Storchi-Bergmann & Cid Fernandes 1999).

These previous results indicate that at least the brightest UV S2 nuclei harbor a starburst. Their UV images suggest that these starbursts have sizes that are similar to those of the Narrow Line Regions (a few 100 pc). However, these results do not demonstrate that starbursts are an ubiquitous part of the Seyfert phenomenon. Cid Fernandes & Terlevich (1995) suggested that circum-nuclear starbursts are a direct consequence of the existence of a molecular torus in Seyfert galaxies, and thus a fundamental part of the Seyfert nuclei. In fact, the torus is the natural place where the star formation can be triggered because it contains a reservoir of molecular gas at a radius of the order of 100 pc.

To more deeply investigate the origin of the FC in S2 nuclei and the role that starbursts play in the Seyfert phenomenon, we present near-ultraviolet to near-infrared spectra of a sample of the 20 brightest S2 nuclei readily accessible from Kitt Peak, with the goal of detecting stellar features characteristic of starbursts. Here, we describe a method to detect young and intermediate massive stars, based on the detection of Balmer and

HeI photospheric lines. The paper is organized as follows. In Section 2 we present the criteria used to select the objects. Section 3 presents the observations and data reduction. Section 4 describes the method followed to detect starburst features at optical wavelengths. Results and interpretation of the data are in Sections 5-8. We discuss our results and their implications in Section 9, and summarize our conclusions in Section 10.

2. Sample selection

The sample comprises the brightest Seyfert 2 nuclei selected from the compilation of Whittle (1992a,b). They have been selected by their nuclear [OIII] λ4959,5007 emission line flux and by their non-thermal radio continuum emission at 1.4 GHz. They all satisfy at least one of the two following criteria: log $F_{[OIII]} \geq$ -12.0 (erg cm^{-2} s^{-1}) and log $F_{1.4} \geq$-15.0 (erg cm^{-2} s^{-1}). The criteria used imply that the sample should be unbiased with respect to the presence or absence of a nuclear starburst. All the objects are classified as spiral galaxies, with 2/3 of the galaxies having a morphological type earlier than Sc (the remaining galaxies do not have a more specific determination)[1]. The redshifts range from 1000 km s^{-1} to 15000 km s^{-1}, with a mean value of 6450 km s^{-1}, giving a mean spatial scale of 420 pc arcsec^{-1} (H_0 = 75 km s^{-1} Mpc^{-1}). At least ten galaxies in the sample are morphologically peculiar. Of these, two galaxies (Mrk 273, Mrk 463E) may be the result of mergers, seven (Mrk 1, Mrk 348, Mrk 477, NGC 5929, NGC 7212 and possibly NGC 7130 and IC 3639) are in gravitational interaction with close companions, and one, Mrk 533, belongs to a Hickson Compact Group and shows signs of tidal interaction. Another three galaxies (NGC 1068, NGC 5135 and Mrk 1066) are members of a groups. The targets and their general properties are summarized in Table 1.

---

[1] The morphological type is from NED.

3. Observations and data reduction

The observations were carried out using the Richey-Chrétien spectrograph attached to the 4m Mayall telescope at Kitt Peak National Observatory during two runs in 1996 February and October. The detector was a T2KB CCD chip with a spatial sampling of 0.7 arcsec/pixel. The slit width was set to 1.5 arcsec for all the observations and it was oriented near the parallactic angle, with the exception of NGC 1068 for which it was set at P.A.=123°. We used two gratings, KPC-007 and BL420, to cover the blue and the red spectral ranges with a dispersion of 1.39 Å/pixel and 1.52 Å/pixel, respectively. Since the edges of the chip are vignetted by the spectrograph camera, the useful spectral ranges are $\sim$ 3400-5500 Å (for the blue) and $\sim$ 6600-9100 Å or $\sim$ 7400-9800 Å (for the red). Typical exposure times were 2×1200 s and 2×1800 s for the blue and red spectral ranges, respectively. The journal of observations is in Table 2.

The reduction of the spectra was performed with the FIGARO data processing software. Bias subtraction and flatfielding were performed in the usual way; a two dimensional wavelength calibration was done using ARC2D (Wilkins & Axon 1991). The spectra were corrected for atmospheric extinction using a curve appropriate for the observatory. The frames were flux calibrated using the standards observed during the same nights with the same set up, but with a 10 arcsec slit width. The frames were corrected for distortion along the spatial direction by using a second order polynomial fit to the spectral distribution of the peak continuum emission of the standard stars, and then applied to the galaxy frames. Sky subtraction was performed in each data frame using the outermost spatial increments where no obvious emission from the galaxy was present. Finally, frames of the same wavelength range were co-added.

In addition to the targets of the sample, we observed the nuclei of three galaxies: NGC 1569 (a dwarf irregular galaxy), NGC 205 (a dwarf elliptical galaxy), and NGC 4339 (an elliptical galaxy). The nuclear spectra of these galaxies show characteristics of young ($\leq$ 10 Myr), intermediate (a few hundred Myr), and old (10-15 Gyr) stellar populations, respectively. Analysis of the spectra of NGC 1569 is presented in González Delgado et al. (1997), of NGC 205 in González Delgado et al. (1999) and Bica, Alloin & Schmidt (1990), and of NGC 4339 in Ho, Filippenko & Sargent (1995). The spectra of these objects are used as templates for the analysis of the Seyfert galaxies.

4. Method for detecting starburst characteristics

Our UV observations of a few objects (those with the brightest UV emission) have shown direct spectroscopic detection of a starburst in the nuclei of these S2 galaxies using strong stellar wind lines like NV λ1240, SiIV λ1400 and CIV λ1550. However, we do not know whether these few galaxies belong to a particular class of Seyfert 2 nuclei or, instead, if starbursts are a fundamental part of the Seyfert phenomenon. To establish the possible connection between the starburst and Seyfert phenomenon we need to detect starburst characteristics in a larger sample of S2 nuclei. Unfortunately, UV spectroscopic observations of this kind of objects are difficult to obtain because only a few of these nuclei have high enough UV surface brightness to be observed spectroscopically with HST. In contrast, near-ultraviolet to near-infrared observations of these objects are more feasible from ground based facilities. Therefore, other diagnostics for starburst characteristics in Seyfert galaxies at optical wavelengths are needed. To search for other diagnostics, first, we examine the morphology of the optical continuum of classical nuclear starbursts.

The optical continuum of classical starburst galaxies is dominated by O, B and A stars. The spectra of young and intermediate mass stars are characterized by strong hydrogen Balmer and neutral helium absorption lines, and with only weak metallic lines (Walborn & Fitzpatrick 1990). The detection of these stellar features at optical wavelengths is difficult because H and HeI absorption features are coincident with strong nebular emission-lines that mask them. However, the higher-order terms of the Balmer series and some of the HeI lines are detected in absorption in many starburst galaxies (Storchi-Bergmann, Kinney, & Challis, 1995) and in the spectra of giant HII regions (e.g. NGC 604, González Delgado & Pérez 2000). These features can be seen in absorption because the strength of the Balmer series in emission decreases rapidly with decreasing wavelength, whereas the equivalent width of the stellar absorption lines is constant or increases with wavelength (González Delgado, Leitherer & Heckman 1999). Thus, the net effect is that Hα, Hβ and Hγ are mainly seen in emission (but they can also show absorption wings superposed on the nebular emission), but the higher-order terms of the series are seen mainly in absorption. A similar effect occurs for the HeI lines, with HeI λ3919, HeI λ4026, HeI λ4388 and HeI λ4922 being more easily detected in absorption. Thus, a method to infer the presence of a starburst can be through the detection of the higher order terms of the Balmer series and the HeI lines in absorption.

In fact, three (NGC 5135, NGC 7130 and IC 3639) of our four S2 that show stellar wind resonance lines in the UV, also show the higher order terms of the Balmer series and HeI (λ3819, 4387 and 4922) in absorption (GD98). These results thus prove that the high order lines of the Balmer series and HeI photospheric lines constitute a good indicator of the presence of massive stars in S2 nuclei. In the other object, Mrk 477, that also shows stellar wind resonance lines in the UV, the Balmer and HeI lines are overwhelmed by the corresponding nebular lines in emission. This implies that this method will not directly detect the existence of massive stars in those nuclei for which the nebular lines are strong and the starburst continuum is weak; thus, a lower limit to the real fraction of objects that show starburst characteristics will be inferred with this method. On the other hand, Mrk 477 shows very broad emission at 4680 Å due to Wolf-Rayet stars. Starbursts go through the Wolf-Rayet phase when stars more massive than 40 M$\odot$ evolve from the main sequence a few Myrs after the onset of the burst.

Another important result from the analysis of the optical spectra of these four S2 nuclei is that the metallic stellar lines due to old, cool stars are very diluted toward the nucleus. As pointed out by CF98, a strong dilution of these lines happens only when the Seyfert nucleus shows starburst characteristics.[2]

Thus, our method to infer the existence of starbursts in S2 galaxies is based mainly on the detection of: 1) The higher order of the Balmer series in absorption and HeI lines; 2) Wolf-Rayet features at optical wavelengths; 3) strong dilution of the metallic lines toward the nucleus.

5. Results and interpretation

5.1. General considerations

In this and the following two sections, we present the general results obtained from the analysis of the spectra observed in the blue spectral range. The techniques used to determine the stellar population in the nuclei of the S2 of our sample and the possible contribution of the FC are these:

1) We compare the nuclear spectral energy distribution and the strength of the stellar lines with those in the spectra of the templates that we observed (NGC 205, NGC 1569, and NGC 4339) and with off-nuclear spectra corresponding to the circumnuclear region of

---

[2] A change in the metallicity of the stellar population will also decrease the equivalent width of the metallic lines; however a strong dilution of these lines is more probably associated to a change of the age of the nuclear stellar population than to metallicity, because the metallicity will increase toward the nucleus when there is a gradient.

the galaxy (section 5.2).

2) We trace the spatial distribution of the equivalent widths (Ew) of the stellar metallic lines near the nucleus (section 5.3).

3) We model the photospheric HeI and Balmer lines with evolutionary synthesis models (section 5.4).

To perform this analysis we have extracted one-dimensional spectra from the two-dimensional frames. For the extractions, we use the spatial distribution of the continuum at 4550 Å along the slit. In a few objects, the maximum of the continuum is not coincident with the maximum of the distribution of nebular lines. The nuclear spectrum corresponds to the central 3 pixels ($\sim$ 2 arcsec) around the maximum of the continuum. The number of off-nuclear spectra varies from 2 in Mrk 78 and Mrk 463E to over 30 in NGC 1068. These spectra cover a distance that ranges from $\pm$2 arcsec to $\pm$60 arcsec. In these extractions, we add 3 or more pixels to get a signal to noise (S/N) in the continuum better than 15. At the nucleus, the S/N is always better than 30. To measure the strength of the stellar lines we have followed the method of CF98 that consists of determining a pseudo-continuum in selected pivot-wavelengths and measuring the equivalent widths (Ew) of the stellar absorption lines integrating the flux under the pseudo-continuum in defined wavelength windows. For the metallic lines, we use the same as CF98 (for CaII K 3908-3952 Å and G band 4284-4318 Å) and for the H Balmer and HeI lines those defined by González Delgado et al. (1999). We do not include in our analysis CaII H and MgI+MgH because these lines can be strongly affected by nebular emission (CaII H by Hϵ and [NeIII] and the MgI+MgH by FeII). The pivot-wavelengths that we use are at 3780, 3810, 3910, 4015, 4140, 4260, 4430, 4800, 4905 and 4935 Å.

A glance at the nuclear spectra reveals that our targets show a variety of stellar population properties, but according to their general continuum morphology they can be grouped in four classes: 1) objects that have stellar absorption features that are strongly diluted at the nucleus; 2) objects in which the stellar lines are similar to those of an old stellar population; 3) objects in which the stellar lines are similar to a young and intermediate age stellar population; 4) objects in which the stellar lines are similar to an intermediate age stellar population.

The detection and characterization of a young or intermediate age population will be most difficult in those cases in which the spectrum is dominated by light from old stars, and those cases in which the nebular emission-lines are very strong (and will therefore fill in the relevant stellar absorption features). To summarize these constraints, and to illustrate the above classification scheme, in Figure 1 we plot the strength of a nebular emission-line (Ew(Hβ)) versus the strength of the tracer of the old stars ((Ew(G band)). The nuclei of groups 1 and 2 are located in different places of the plot than nuclei belonging to the third and fourth groups. However, we also found transition objects between groups.

5.2. Empirical comparisons

In this sub-section we report the results of the first technique described above. It allows us to derive the general characteristics of the stellar population and to infer whether it is similar to that of an elliptical galaxy or, in contrast, to younger stellar systems; and to estimate the possible AGN contribution. We will discuss each of the four classes in turn.

5.2.1. Nuclei with very weak stellar absorption-lines

In this group are Mrk 477 and Mrk 463E. They both have very strong nebular Hβ emission and the stellar lines are very weak. The nucleus of Mrk 477 shows a broad emission feature at 4680 Å (Figure 9 in H97). As has been discussed extensively by H97, the origin of this feature could be due to Wolf-Rayet stars. We rule out the possibility that this feature is scattered HeII λ4686 emission from the hidden S1 nucleus because the polarized spectrum does not show HeII emission, and the degree of polarization is only a few percent (Tran 1995b). Evidence that Mrk 477 harbors a nuclear starburst comes from the detection of the UV resonance wind stellar lines. This detection gives support to the hypothesis that the broad emission feature at 4680 Å is produced by Wolf-Rayet stars. Additional evidence comes from the spectral energy distribution of the nuclear continuum at optical wavelengths, which is well fitted by a starburst in the Wolf-Rayet phase plus the contribution of the nebular Balmer recombination continuum (see Figure 6 in H97). However, the Balmer and HeI photospheric absorption features in the nuclear spectrum of Mrk 477 are completely overwhelmed by the corresponding nebular lines. In contrast, a circumnuclear spectrum of Mrk 477 extracted 2 arcsec from the peak of the optical continuum shows the higher order terms of the Balmer series in absorption. The spectrum is also similar to that of the companion galaxy of Mrk 477, that according to its nebular line emission can be classified as a LINER (De Robertis 1987), but its continuum shows a starburst morphology (Figure 2). We will show later in Section 7 that the stellar population of the circumnuclear region of Mrk 477 is dominated by young and intermediate mass stars. However, evidence for the Balmer lines in absorption in the nuclear spectrum of Mrk 477 is found indirectly. Using the profile of the nebular emission of Hβ in the nucleus, the Balmer decrement and the reddening that affects the ionized gas (E(B-V)= 0.23, H97), we have predicted the intensity of the nebular emission of H8-H10. We have subtracted these lines from the nuclear spectrum, and the resulting spectrum has H9 and H10 in absorption. The Ew of these lines are $\sim$ 2 Å, which is the typical value predicted for very young starbursts (González Delgado et al. 1999). Thus, we conclude that the circumnuclear region of Mrk 477 contains stellar features characteristic of a young and intermediate age population.

As it has been pointed out before, the optical nuclear spectrum of Mrk 436E is very similar to the nuclear spectrum of Mrk 477. Mrk 463E shows also a broad emission feature at 4680 Å (Figure 3). To investigate the origin of this feature we have examined its polarized optical spectrum. It shows broad Hα, Hβ and FeII emission, but it does not show HeII λ4686 broad emission (Tran 1995b). Thus, as in Mrk 477, we can rule out scattered light from the hidden S1 nucleus as the origin of the broad emission at 4680 Å. However, this result by itself cannot prove whether or not there is a starburst in the Wolf-Rayet phase in the nucleus of Mrk 463E. To look for evidence of the evolutionary state of the stellar population in Mrk 463E, we have predicted the intensity of H8-H10 in emission as we did for the nuclear spectrum of Mrk 477. In this case the higher order Balmer series lines are only marginally detected, but with Ew's that are similar to the case of Mrk 477. The detection is not firm because the continuum in the circumnuclear region of Mrk 463E is fainter than in Mrk 477 and the S/N is not good enough to safely infer the stellar population. While the strong similarity of the spectra of Mrk 477 and Mrk 463E is very suggestive of a starburst in the latter, it will have to be confirmed at space-UV wavelengths.

In the absence of space-UV spectroscopy, images can alternatively provide indirect evidence of a nuclear starburst in Mrk 463E through the morphology of the emission. We have observed Mrk 463E with HST and the Faint Object Camara (FOC) with the F/96 relay that gives a spatial scale of 0.0014 arcsec/pixel. We used the F210M filter, because its bandpass does not include any strong emission lines and so is dominated by the UV continuum (Figure 4). Mrk 463E shows a UV knot which nature is unknown, but most of its UV flux comes from 1 kpc extended emission whose morphology is suggestive of the scattered light from the hidden S1 nucleus known from spectropolarimetry. Therefore, we found that the UV morphology of Mrk 463E looks different from that of the other S2 nuclei that directly show starburst characteristics in their UV spectra (see Figure 1 in H97 and Figures 4-7 in GD98). Thus, the origin of the continuum and the broad emission at 4680 Å is still an enigma. Mrk 463E is a very challenging object and HST+STIS observations will help to further probe the origin of the broad emission feature at 4680 Å and the FC.

5.2.2. Nuclei with a dominant old stellar population

In 8 of the objects (Mrk 3, Mrk 34, Mrk 348, Mrk 573, NGC 1386, NGC 2110, NGC 5929 and NGC 7212) the stellar lines are similar to those of an old population. The equivalent width (Ew) of the CaII K (λ3933) and the G band (λ4300) ($\geq$ 8 Å and $\geq$ 4 Å, respectively) are larger than those in our young (1.8 Å and 1.5 Å in NGC 1569) and intermediate age population templates (5.6 Å and 3.9 Å in NGC 205). However, the lines are weaker than in the elliptical galaxy (14 Å and 7.5 Å in NGC 4339). In particular, in three of these S2 nuclei (Mrk3, NGC 7212 and Mrk 34) the stellar lines are significantly diluted with respect to the elliptical galaxy. Figure 1 shows that these 8 nuclei are distributed along a line in the plane Ew(Hβ)-Ew(CaII K), where the stellar lines are weaker in those objects with larger Ew of Hβ emission. This relationship suggests that the S2 nucleus that has a more powerful engine source (thus, it has stronger nebular emission) can also have stronger contributions of the scattered or reprocessed light from the hidden nucleus, and in consequence the stellar lines are more diluted with respect to those in typical old stellar systems. Alternatively, as suggested by S98, the stellar lines can be weaker than those in an elliptical galaxy because the stellar bulge population in these objects has a larger fraction of intermediate age stars or the metallicity is lower than in the elliptical galaxy. However, the metallicity is not the relevant parameter because it is solar or over in the central regions of Seyferts (González Delgado & Pérez 1996; Storchi-Bergmann et al 1998), and thus it is similar to the metallicity in elliptical galaxies.

To distinguish between these two alternative solutions we have proceeded in two different ways. First, we fit the continuum distribution with our template elliptical galaxy plus the FC represented by a power-law ($F_\lambda \propto \lambda^{-1}$). Second, we fit the nuclear continuum with an off-nuclear spectrum of the galaxy bulge as a template. The goal is to check whether in this second way, the fit requires the presence of a FC as is required using the elliptical galaxy as a template. In both ways, we add the contribution of the nebular Balmer continuum only if Ew(Hβ) is larger than 20 Å because in weaker nuclei (Ew(Hβ) $\leq$ 20 Å) the nebular continuum contributes less than 2% to the total light at 4800 Å.

The results of the first exercise indicate that all the nuclei in this group are well fitted by the elliptical galaxy plus a power-law that contributes from 0% to 25% to the total light at 4800 Å (the lowest contribution is in the nucleus of NGC 1386 and the largest one is in the nucleus of Mrk 34). The results of the second exercise indicate than in half of these objects (Mrk 348, NGC 1386, NGC 2210 and NGC 5929) the fit does not need the contribution of a power law because the stellar lines are similar to those in their corresponding off-nuclear spectrum and the nuclear continuum distribution is redder than in the off-nuclear spectrum. Therefore, the small dilution of the nuclear stellar lines in Mrk 348, NGC 1386, NGC 2210 and NGC 5929 with respect to the elliptical galaxy is most probably related to a change of the stellar population with respect to that of NGC 4339. The cause can be a larger contribution of intermediate age stars than in an elliptical galaxy. In the other four nuclei (Mrk 3, Mrk 34, Mrk 573 and NGC 7212) the fit using the elliptical galaxy spectrum is better than that using the off-nuclear spectrum. Thus, the dilution of the stellar lines in these nuclei with respect to the elliptical galaxy is probably related to the presence of scattered light produced by the hidden Seyfert 1 nucleus. Examples of the fits are in Figure 5.

Therefore, we conclude from this analysis that the stellar population of the nuclei of galaxies in this group is, in general, similar to that of an elliptical galaxy but they can also have a larger contribution of intermediate age stars. Thus, the characterization of the nuclear stellar population is important to infer the possible existence of scattered light from the hidden Seyfert source and its contribution to the optical light. The comparison of the nuclear spectrum with the bulge spectrum as well as with galaxy templates can help to provide a good estimate of the FC if it exists.

5.2.3. Nuclei with young and intermediate age populations

HeI and/or the higher order terms of the Balmer series have been directly detected in 6 nuclei of the sample. They are: Mrk 273, Mrk 1066, Mrk 1073, NGC 5135, NGC 7130 and IC 3639 (see Figure 6). They have relatively weak nebular emission (Ew(H$\beta \leq 25$ Å) allowing the direct detection of some photospheric Balmer and HeI lines. They show the G band and CaII K lines weaker than 4 Å and 7 Å, respectively. Thus, the stellar population of these nuclei is very different from the stellar population in elliptical galaxies and it is more similar to young and intermediate age stellar systems. A comparison of the nuclear spectra with the corresponding off-nuclear spectra indicate that the nuclei of NGC 5135, NGC 7130 and Mrk 1066 are bluer; Mrk 273 and Mrk 1073 have similar colors to their off-nuclear spectra; and the nucleus of IC 3639 is redder than its off-nuclear spectrum. In all the nuclei of this group, the stellar lines are diluted with respect to the off-nuclear spectra. This dilution could be due to the presence of scattered light from the nucleus or by a larger contribution of young stars in the nucleus.

We have tried to fit the spectral distribution of the continuum and stellar features combining the off-nuclear bulge spectra and a power-law, as we did in Section 5.2.2. We found that we need contributions of the FC at 4800 Å of 50 %, 40 % and 30 % for NGC 5135, NGC 7130 and Mrk 1066, respectively (Figure 7). However, this result is not supported by our UV spectroscopic observations of NGC 5135 and NGC 7130. If the FC contributed to the optical light with these large fractions, then the UV continuum of these nuclei would be totally dominated by scattered light from the hidden S1 nuclei, and the spectra would not show any stellar features. In contrast, the UV spectra of NGC 5135 and NGC 7130 clearly show strong resonance lines formed in the wind of massive stars; the UV wavelengths are totally dominated by a very powerful and young starburst (GD98). The reason why the optical continuum can be fitted by the off-nuclear spectrum plus the contribution of the power-law is because young starbursts have spectral energy distributions that mimic the shape of a power-law (Cid Fernandes & Terlevich 1995). Therefore, these results point to an alternative interpretation, namely, that young powerful starbursts contribute significantly to the optical light of the nuclei of NGC 5135, NGC 7130 and Mrk 1066.

The optical continua of the nuclei of Mrk 273 and Mrk 1073 are well fitted by the off-nuclear spectra, but their stellar lines are weaker in the nuclei. These results also suggest that young starbursts also contribute to the optical nuclear light of Mrk 273 and Mrk 1073, but they are very reddened. Therefore, these red starbursts contribute by diluting the stellar lines but do not make the nuclear spectra very blue with respect to the off-nuclear spectra.

In this group, IC 3639 has the nucleus with the strongest G band and CaII K lines; however the Ew of Hβ in emission is similar to other objects in this group. The strength of its metallic stellar lines are similar to those in the spectrum of an intermediate age population system (e.g. NGC 205). Direct evidence that IC 3639 harbors a nuclear starburst comes from its UV spectrum. As in NGC 5135 and NGC 7130, the UV nuclear spectrum of IC 3639 shows stellar resonance lines formed in the winds of massive stars (GD98). The starburst in the nucleus of IC 3639 is dusty and less luminous than those in NGC 5135, NGC 7130 and Mrk 477. Therefore, we expect that its contribution to the optical light is lower than in the latter objects. A starburst weaker than in NGC 5135 and NGC 7130 will also explain why the metallic stellar lines in IC 3639 are less diluted than in NGC 5135 and NGC 7130 and why the spectrum is not so blue. We will see later that the

Balmer absorption lines are fitted with the contributions of a young and an intermediate age population.

In Mrk 533 and Mrk 1 the stellar lines due to old, cool stars are similar in strength to the objects in the above group, suggesting a similarly strong contribution from young/intermediate age stars. However, the nebular line emission in these nuclei is substantially stronger, making the direct detection of the stellar Balmer absorption lines more difficult. However, we do find evidence for the existence of young and intermediate age stars in the circumnuclear region of these galaxies, as we now discuss in detail.

The metallic stellar features in Mrk 533 (EW(G band)= 1.9 Å and EW(CaII K)= 3.8 Å) are very diluted with respect to those of an elliptical galaxy, and its continuum is bluer than that of elliptical galaxies. We find that it is not possible to adequately fit the spectral energy distribution of the optical continuum with only a combination of an elliptical galaxy plus a power-law. The strength of the stellar lines is similar to the more diluted objects of the third group (e.g. of NGC 5135, NGC 7130 and Mrk 1066). This suggests that the stellar population and the spectral energy distribution in Mrk 533 could be better reproduced by a young or intermediate age stellar population. A comparison with the continuum distribution of NGC 205 shows that the nucleus of Mrk 533 is bluer than NGC 205; thus, a contribution of a power-law or/and a younger stellar population than that of NGC 205 is required to fit the shape of continuum in the nucleus of Mrk 533. In fact, a power-law that contributes 15% of the total light at 4800 Å plus the spectrum of NGC 205 can reproduce the continuum, except below 3750 Å where Mrk 533 is bluer than the composite spectrum. However, this result does not prove the existence of scattered AGN light in the nucleus of Mrk 533, because a combination of two off-nuclear spectra extracted $\sim$ 5 arcsec from the peak of the continuum also fits the nucleus of Mrk 533 well if the off-nuclear template is reddened by E(B-V)= 0.1. This template shows Balmer absorption lines, indicating that an intermediate age population contributes significantly to its optical light. However, the nucleus of Mrk 533 has stronger nebular Balmer lines than the other nuclei of the third group, and the direct detection of the photospheric lines is more difficult than in the cases of Mrk 273, Mrk 1066, Mrk 1073, NGC 5135, NGC 7130 and IC 3639.

To detect indirectly the Balmer lines in absorption, we have predicted the intensity of the Hδ-H10 by scaling the profile of Hβ using the Balmer decrement and the extinction, E(B-V)= 0.3, derived from the ratio Hγ/Hβ. We subtract the predicted nebular lines from the nuclei of Mrk 533 and the resulting spectrum shows absorption features that are very similar to those in the off-nuclear template (Figure 8).

The nucleus of Mrk 1 shows metallic stellar features that are very diluted with respect to those in an elliptical galaxy and are similar to objects in the third group. Its continuum distribution cannot be fit by the combination of a power-law and an elliptical galaxy because the power-law has to contribute 40% of the total light at 4800 Å to reproduce the shape of the continuum, and the stellar lines in the composite fit spectrum are then weaker than in the nucleus. However, the nuclear spectrum can be fitted by an off-nuclear spectrum if it is reddened by E(B-V)= 0.2. The spectrum is extracted from 3 arcsec off the continuum peak at 4450 Å. The shape of the continuum and the stellar features in the circumnuclear spectrum are similar to a spectrum dominated by an intermediate age population, with the high order Balmer series in absorption. However, these lines are not detected in absorption in the nuclear spectrum because the nebular contribution is very strong. Mrk 1 has EW(Hβ) $\sim$ 70 Å, and is one of the nuclei with the strongest nebular Balmer emission (after Mrk 477 and Mrk 463 E).

To indirectly detect these absorption lines, we predict the nebular Hδ-H10 in the same way as we did in Mrk 477, Mrk 463E and Mrk 533. We subtract the nebular lines from the nuclear spectrum of Mrk 1. The resulting spectrum has absorption features that are very similar to those in the off-nuclear spectrum (Figure 9).

We also find (as in Mrk 477 and Mrk 463E) that there is a weak, very broad emission feature underlying the HeIIλ4686 nebular emission line in Mrk 1 (Figure 10). As in the other cases, we cannot prove that this feature is due to a substantial population of Wolf-Rayet stars. We can however rule out an origin due to scattered AGN light, since this broad bump is not seen in the polarized-flux spectrum.

To conclude, our analysis strongly suggests that the nuclear stellar population of Mrk 533 and Mrk 1 has an important contribution of young and intermediate mass stars, even though the direct spectroscopic signature of these stars is not clear.

5.2.4. Nuclei with a pronounced intermediate age population

The metallic lines in the nucleus of Mrk 78 are diluted with respect to those in an elliptical galaxy and are similar to those in NGC 205. The nucleus also shows relatively weak nebular Balmer lines, facilitating the detection of the Balmer absorption lines. In fact, Hδ and Hϵ show a hint of absorption. Below 3900 Å, the spectrum shows Balmer absorption features, but they do not correspond to those of a young (a few Myr old) age population. Thus, the stellar population in Mrk 78 consists of a mixture of old and intermediate age stars. Indeed, a combination of a 1 Gyr old (A and F star dominated) population with that of an elliptical reproduces well the continuum shape and the strength of the stellar lines (Figure 11).

The nuclear spectrum of NGC 1068 corresponds to the central 2 arcsec around the continuum peak. This spectrum shows that the metallic stellar lines are very diluted with respect to an old stellar population. A combination of an elliptical galaxy and a power-law can reproduce the continuum shape if the power-law contributes with at least

35% of the total light at 4800 Å, but this combination cannot fit the observed stellar lines. A comparison of the nuclear with an off-nuclear spectrum, extracted 4 arcsec from the continuum peak, indicates that the nucleus has also weaker metallic lines than the off-nuclear spectrum. Thus, the contribution of the scattered light from the hidden S1 nucleus can contribute to the dilution of these the lines. A combination of this off-nuclear spectrum plus a power-law that contributes 10-15% to the total light at 4800 Å fits it well (Figure 12). An inspection of this off-nuclear spectrum shows that the stellar population there has an important contribution of intermediate age stars (see section 5.3).

5.3. Spatial variation of the stellar lines

The spatial distribution of the Ew of the metallic lines around the nucleus allows us to estimate the possible variations of the stellar population as a function of distance from the nucleus. That is, the presence of a younger stellar population will produce a strong dilution of the stellar lines toward the nucleus. However, dilution of the stellar lines can also be caused by scattered light from the hidden S1 nucleus. But the dilution factor, together with the stellar characteristics of the nuclear and off-nuclear spectra, can point to one of these two alternatives.

5.3.1. Nuclei with very weak stellar absorption-lines

In Mrk 477 the spatial distribution of the G band and the CaII K lines shows a deep dip in the Ew of the lines at the nucleus (Figure 13). Comparing to the values out of the nucleus, the dilution of the light of old stars is $\sim 70\%$. This strong dilution of the stellar lines at the location of the continuum peak cannot be produced by a power-law, because if that were the case the UV light would have to be totally dominated by FC. On the contrary, we found that the UV light is produced by a starburst in the nucleus of Mrk 477 (H97).

In Mrk 463E we have extracted two off-nuclear spectra at ±2 arcsec from the nucleus. The Ew of the stellar lines in these off-nuclear spectra are 2.7 Å and 1.5 Å for the CaII K and the G band, compared to 0.9 Å and 0 Å, respectively, on the nucleus. Thus the metallic lines are significantly more diluted in the nucleus.

5.3.2. Nuclei with a dominant old stellar population

The plot of the EW of the metallic lines as a function of the distance from the nucleus shows that the variation of the strength of the stellar lines in the nucleus and circumnuclear region of these galaxies is small or null (Figure 14). The dilution factor is $\leq 10\%$. The exception to this bevavior is Mrk 3, where the stellar lines at the nucleus show a significant dilution with respect to the circumnuclear region (Figure 14). The estimated dilution factor is $\sim 25\%$.

The lack of any significant dilution in Mrk 573, Mrk 34 and NGC 7212 is surprising, given that the continuum spectral energy distribution in these nuclei required the contribution of a power-law. As pointed out by S98, the presence of an extended scattered continuum could be the explanation, because it can contribute equally to the nuclear and to the off-nuclear spectra, thus keeping the EW of the lines approximately at the same values.

5.3.3. Nuclei with young and intermediate age populations

In the galaxies of this group, the Ew of the metallic stellar lines shows a spatial variation, that indicates that there is a significant change of the stellar population with distance from the nucleus. The metallic lines are diluted with respect to the off-nuclear spectra; in particular, the dilution is very strong in those nuclei that have bluer colors than their surroundings (Mrk 1066, NGC 5135 and NGC 7130). The dilution factor ranges between 45% and ∼ 10%, the stronger dilution corresponding to NGC 5135 and the lower to IC 3639. The UV spectra of IC 3639 and NGC 5135 both show strong evidence for the existence of a nuclear starburst in these two galaxies. Thus, the significant difference between the dilution factor in NGC 5135 and IC 3639 could be related to the existence of a more powerful starburst in NGC 5135 than in IC 3639. Examples of the spatial variation of Ew are in Figure 15.

5.3.4. Nuclei with a pronounced intermediate age population

In Mrk 78 we have extracted two off-nuclear spectra that are at ±2 arcsec from the nucleus. Even we have only three points, the plot of Ew of the stellar lines does not show a variation of the strength of the stellar lines with the distance from the nucleus.

In contrast, in NGC 1068 we have traced the spatial distribution of the strength of the stellar lines out to ±60 arcsec from the nucleus. There is a significant change of the Ew of the lines with the distance. The nuclear population is strongly diluted with respect to the population at ±5 arcsec. Values of the Ew of the lines at ±10 arcsec are similar to those of the nucleus; however, the dip of the strength of the lines is due to the presence of young massive stars in the circumnuclear ring (Figure 16).

5.4. Modeling the Balmer absorption lines

In the previous analysis we have found that six nuclei (Mrk 273, Mrk 1066, Mrk 1073, NGC 5135, NGC 7130, and IC 3639) have strong Balmer absorption lines. These lines are also detected in the circumnuclear regions in another three galaxies (Mrk 533, Mrk 1, and Mrk 477) and in their nuclei when the contribution of the nebular emission is subtracted. The strength of these and the metallic lines indicates that the stellar population is dominated by young and intermediate mass stars. We also found that the circumnuclear region of NGC 1068 and the nucleus of Mrk 78 show Balmer lines, but the strength of the Balmer and metallic lines suggests that the stellar population in these two objects has an important contribution of intermediate age stars.

To estimate the contribution of young and intermediate mass stars to the optical light of these objects, we use the technique of stellar evolutionary synthesis. The models predict the profile of the HeI and Balmer absorption lines for single metallicity stellar population as a function of the age, assuming an initial mass function (see González Delgado et al. 1999 for details). These models use a stellar library that comprises synthetic spectra of stars that were generated with stellar atmosphere models (see González Delgado & Leitherer 1999 for details). We have updated these models to predict several spectral ranges that were not computed previously. Thus, these new models predict the CaII H and K, Hϵ and the spectral range around the G band. The stellar spectra reproduce well the stellar lines with effective temperature larger than 6000 K; thus, they can be used to predict the photospheric stellar lines of populations younger than a few Gyr old.

To avoid having to introduce the extinction as an additional free parameter in the fit to the S2 spectra, we use normalized spectra, by dividing by the continuum resulting of fitting a line between two consecutive pivot wavelengths (defined in section 5). A general result is that the stellar population cannot be described by only two components, for example an old (10-15 Gyr) plus a young or intermediate population. Thus, the fit of the metallic and Balmer lines requires three components: a young, an intermediate and an old population. We take for the young population an instantaneous burst 3 Myr old, for the intermediate age population a combination of three bursts of 200, 500 and 1000 Myr old (roughly equivalent to a burst lasting 800 Myr commencing 1 Gyr ago), and for the old population the elliptical template. To show the validity of the process followed, we present first the result of fitting our intermediate age stellar population galaxy template NGC 205. We find a good fit with a combination of intermediate age (0.2 to 1 Gyr) plus the elliptical galaxy if they contribute to the light at 4800 Å with 70% and 30%, respectively (Figure 17). This solution reproduces quite well not only the strength of the lines but also the shape of the continuum. It agrees with that found by Bica et al. (1990). We report the results of the fit by grouping the objects according to the contributions of the young and old populations. First, we report the results of fitting the nuclear spectra (Figure 18), and then the off-nuclear spectra of Mrk 1, Mrk 533, NGC 1068 and Mrk 477. The plots are in Figure 19.

5.4.1. The nuclei of NGC 5135 and NGC 7130

These spectra show very weak metallic lines and strong Balmer and HeI (λ3819 and λ4026) in absorption. They both require an important contribution of a young stellar population. The strong dilution of the G band and the CaII K line indicates that the old population contributes very little to the optical light ($\sim$ 10%). The dilution of these lines is produced by the contribution of a young and an intermediate-age stellar population that provide 50% and 40%, respectively, of the total optical light (see Figure 18a).

5.4.2. The nuclei of Mrk 273, Mrk 1066 and Mrk 1073

The strength of the metallic lines requires a contribution of the old population that is larger than in NGC 5135 and NGC 7130; it is between 20% (for Mrk 1066) and 30% (for Mrk 273 and Mrk 1073). The strength of the Balmer lines requires an intermediate population that contributes 50%, and a young burst that contributes 30% (in Mrk 1066) and 20% (in Mrk 273 and Mrk 1073) (see Figure 18b and c). However, we have noticed that a similar fit is obtained if we substitute the contribution of the young stellar population by the contribution of a power-law that provides 30% and 20% of the total optical light.

5.4.3. The nucleus of IC 3639

IC 3639 has the nucleus with the strongest metallic lines of its group, and the fit of the lines requires a contribution of the old stellar population that is the largest fraction, 40% of the total optical light. The intermediate and the young stellar population contribute 40% and 20% of the optical light, respectively (Figure 18d).

5.4.4. The nucleus of Mrk 78

As we already explained above, the nucleus of Mrk 78 shows Balmer absorption lines, but they are weaker than those expected for an intermediate age population. The strength of the G band and the CaII K lines suggests that the contribution of the old population is important. The combination of the intermediate age population with the elliptical galaxy fits the nuclear spectrum reasonably well if each population contributes half of the total optical light (Figure 10). However, from the fit of the stellar lines, we cannot rule out that 10% of the total light could be provided by a power-law.

5.4.5. Off-nuclear spectra of Mrk 1 and Mrk 533

The nuclei of these two objects have the stellar Balmer lines filled in by the corresponding nebular lines. However, as we have already seen, the nuclear spectra show the absorption features when the nebular contribution is subtracted. The resulting spectra have features similar to the circumnuclear spectra with characteristics of an intermediate age population. To perform the fit we use the off-nuclear spectra of Mrk 1 extracted 3 arcsec from the continuum peak and one of Mrk 533 at 5 arcsec. Both spectra are well fitted by a combination of young, intermediate and old populations that contribute 20%, 40% and 40%, respectively (Figure 19a).

5.4.6. Off-nuclear spectra of NGC 1068

We have fitted two circumnuclear spectra of NGC 1068. One is the average of two spectra (extended 2 arcsec) extracted at ± 4 arcsec of the continuum peak at 4450 Å, that represents the off-nuclear stellar population of NGC 1068. We call it the bulge spectrum. The second spectrum corresponds to the circumnuclear HII ring and it is extracted from 8 arcsec of the continuum peak and it extends 7 arcsec. We call it the HII ring spectrum.

The bulge spectrum is well fitted by combining an intermediate age population with the elliptical galaxy, each contributing half to the total optical light (as in Mrk 78). A power-law that contributes 10% and the rest provided by the intermediate age plus the old population is also acceptable (Figure 19b). The HII ring spectrum requires the contribution of three populations, a young burst, an intermediate and an old stellar population. They contribute 40%, 30% and 30% of the total optical light, respectively (Figure 19c).

5.4.7. Off-nuclear spectrum of Mrk 477

We take an off-nuclear spectrum 1.5 arcsec from the continuum peak and extended by 2 arcsec. The spectrum clearly shows the higher order terms of the Balmer series in absorption, and the G band and Ca II lines. We fit also the spectrum with the contribution of three components, a young burst, an intermediate and an old stellar population, that contribute 30%, 40% and 30% of the total optical light respectively, (Figure 19d).

5.5. CaII triplet: general results

The most prominent stellar feature in the red/near-IR region is the CaII triplet (λ8498, 8542, 8662). These lines are detected in absorption in many Seyfert galaxies (Terlevich et al. 1990; Nelson & Whittle 1995), in most of the nuclear starburst galaxies (Storchi-Bergmann et al, 1995) and in the spectra of young stellar clusters (Bica, Santos & Alloin 1990; González Delgado et al 1997). These lines are formed in the photospheres of asymptotic giant branch, red giant and red-supergiant stars (Díaz, Terlevich & Terlevich 1989). They are very strong in starbursts with ages between 10 and 20 Myr (Mayya 1997; García-Vargas, Bressan & Mollá 1998) due to the evolution of massive stars to the red supergiant phase.

We have observed our sample in the red to detect the CaII triplet and to estimate the possible dilution of these lines with respect to normal galaxies. We also observed our template galaxies. Three of our targets (Mrk 533, NGC 5135 and IC 3639) could not be observed. The two most distant objects of our sample (Mrk 463E and Mrk 34) were affected too strongly by the strong sky emission at 9000 Å and longer wavelengths. However, in the remaining objects the lines are very strong. We have measured the equivalent widths of the lines using the line windows defined by Díaz et al (1989); the values are in Table 3.

We found that the nuclei that belong to the second group (i.e. those with a stellar continuum dominated by an old stellar population) show a CaII triplet strength that is very similar to the elliptical galaxy NGC 4339 (Figure 20a). The exceptions to this behavior are Mrk 3 and NGC 7212. They both have CaII triplet equivalent widths lower than the elliptical galaxy and than the rest of the nuclei of this group. These two nuclei have very strong nebular emission and the blue stellar lines are diluted with respect to an old population. We found that the dilution in the blue spectral range is due to the contribution of scattered light from the hidden Seyfert nuclei plus the nebular continuum. Thus, these two contributions can also dilute the CaII triplet. On the other hand, these two nuclei have very strong Balmer nebular emission. Thus, Pa13 and Pa16 that fall at the same wavelengths as CaII λ8452 and CaII λ8662 can partially fill in the absorption lines. Mrk 3 and NGC 7212 also show a broad emission feature at 8600 Å that is produced by emission of [ClII] λ8580, Pa 14, and [FeII] λ8617.

The nuclei that show the higher order Balmer series in absorption also show strong CaII triplet lines that have equivalent widths similar to those of NGC 205 (Figure 20b). The nucleus of Mrk 1 also has the CaII triplet with strength similar to that of NGC 205. However, these lines in NGC 205 are only slightly weaker than those in the NGC 4339. The CaII triplet has been detected also in the nuclear spectrum of Mrk 477 (one of the two objects with a blue spectrum that does not show any stellar features) with a strength similar to that in NGC 205.

6. Discussion

6.1. Properties of the sample in the infrared

The infrared emission from S2 galaxies comes three different sources. Dust in/near the central engine (probably associated with the dusty obscuring torus) will be heated by a hidden S1 nucleus and emit primarily in the near- and mid-IR. Dust heated by a hot starburst population will emit primarily in the far-IR, as will the dust heated by the normal stellar radiation field in the large-scale ISM. In this section, we will assess the origin of the infrared emission in our sample and compare the infrared properties of the S2 nuclei with predominantly old and young/intermediate age stellar populations. The infrared dominates the broad-band spectral energy distributions of nearly all our galaxies. The total infrared luminosity estimated with the fluxes of all four IRAS bands (Sanders & Mirabel 1997) ranges from 3×10^9 to 1.2×10^{12} L$\odot$ for our sample. All the galaxies, except NGC 1386, have an infrared luminosity larger than the typical value for a normal spiral (10^{10} L$\odot$), and the log-mean luminosity of our sample is 10^{11} L$\odot$. Therefore, most galaxies in our S2 sample can also be classified as Luminous Infrared Galaxies.

The objects in our sample were selected based on the emission-line and/or radio continuum fluxes of their nuclei. They are therefore amongst the brightest S2 nuclei of the Whittle (1992) compilation. This is also true in the mid-IR. In particular, all the galaxies in the sample are also powerful infrared emitters at 12 μm, which Rush, Malkan, & Spinoglio (1993) argue is the least-biased waveband for selecting Seyfert nuclei. The 12 μm luminosity for our sample (νP_ν), ranges from 6×10^8 to 2×10^{11} L$\odot$. Most of the galaxies have $L_{12} \geq 10^{10}$ L$\odot$, and only three galaxies (NGC 1386, NGC 2110, and NGC 5929) have L_{12} significantly lower than 10^{10} L$\odot$. Bonatto & Pastoriza (1997) have compiled the IRAS fluxes of a large sample of Seyfert galaxies, and they found that, for the S2, the L_{12} distribution peaks at 10^{10} L$\odot$. Thus, the nuclei selected in our sample are amongst the most powerful and brightest S2 at mid-infrared wavelengths. The S2 in our sample are much more luminous in the mid-IR than normal galaxies. According to the luminosity function presented by Rush, Malkan & Spinoglio (1993), only a small fraction of normal galaxies have $L_{12} \geq 10^{10}$ L$\odot$. We found for our sample that L_{12} correlates with the power of the AGN as measured by both the [OIII] λ5007 luminosity and the 1.4 GHz non-thermal nuclear radio continuum power. These results suggest that (contrary to normal galaxies, where the 12 μm flux is emitted mostly by small grains in the large-scale interstellar medium) the 12 μm continuum in our S2 sample is emitted by warm dust heated by the AGN.

These results imply that our sample is representative of the brightest and most powerful S2 nuclei in the local universe (regardless of how the nuclear luminosity is measured). In particular, even though many of the galaxies in our sample were originally discovered by their ultraviolet excess (e.g. in the Markarian surveys), most of them are also abnormally strong mid-infrared and radio emitters. Therefore, we can conclude that our sample is not biased towards nuclei that have a starburst, as could be thought *a priori* for objects initially discovered by their ultraviolet emission.

We can compare the nuclear luminosities of the S2 nuclei with predominantly old and young/intermediate age stellar populations. The 12 μm luminosity of the nuclei whose optical continuum is dominated by an old stellar population (Mrk 3, Mrk 34, Mrk 348, Mrk 573, NGC 1386, NGC 2110, NGC 5929, and NGC 7212) has a mean value of log $L_{12}/L_\odot = 9.84\pm0.19$. In contrast, those nuclei that have a young and intermediate age population (Mrk 1, Mrk 273, Mrk 477, Mrk 533, Mrk 1066, Mrk 1073, NGC 5135, NGC 7130, and IC 3639) have a mean log $L_{12}/L_\odot = 10.37\pm0.11$. Thus, we find that the S2 in our sample that show starburst characteristics may be more powerful AGN (at the 2.5σ significance level). To test this further, we have compared the luminosities of the [OIII] emission-line and the 1.4 GHz nuclear nonthermal radio emission in the two sub-groups. The S2 group with a dominant old population has a mean value log $L_{[OIII]}$/erg s^{-1} = 41.51±0.32 compared to 41.55±0.21 for the S2 nuclei with young/intermediate age populations. The S2 group with a dominant old population has a mean value log $L_{1.4}$/erg s^{-1} = 38.63±0.34, compared to 39.09±0.16 for the S2 nuclei with young/intermediate populations. In all three comparisons, the younger stellar populations are associated with more luminous AGN, but the statistical significance ranges from nearly zero to marginal. Larger samples, especially those that better sample the highest luminosity S2 nuclei, will be required to confirm this.

A stronger difference between the old and young/intermediate S2 nuclei is found if we compare the far-infrared (40 to 120 μm) luminosity. The mean value in the first group of nuclei (old stars) is log $L_{FIR}/\mathrm{L}_{\odot} = 10.05 \pm 0.20$. This is significantly lower (3σ) than the emission in galaxies that have nuclei with young and intermediate age stars (log $L_{FIR}/\mathrm{L}_{\odot} = 10.83 \pm 0.17$). This result is very reasonable since the FIR is an excellent tracer of dusty star-formation in galaxies. In the local universe, galaxies with FIR luminosities greater than log $L_{FIR} \sim 10.5$ are almost exclusively starbursts. We find that ∼80% of the young/intermediate S2 nuclei in our sample exceed that threshold, compared to only 25% of the old S2 nuclei. These results suggest that there is a direct connection between the young/intermediate age stars and the population that heats the dust radiating in the far-IR. This has been confirmed quantitatively for the four S2 nuclei studied in detail by GD98.

6.2. Implications for the starburst-Seyfert connection

The detection of the higher order terms of the Balmer series in absorption in the near-ultraviolet spectra in about half of the S2 of the sample, contrasts with the general view that the nuclear spectra of Seyferts are composed of an old stellar population plus the scattered light from the hidden nucleus. The analysis of the near-ultraviolet spectra indicates that young and intermediate age stars are present in the nuclear and circumnuclear regions of 45% of the S2 galaxies of this sample[3] . In an additional 10% the sample, an intermediate age population contributes significantly to the optical light. However, the contributions of young and intermediate age stars change from object to object. We find the largest contributions in the nuclei of NGC 5135 and NGC 7130, both with a fraction of 50%

---

[3] Storchi-Bergmann et al. (2000) have recently presented the analysis of a sample of 20 Seyfert 2 galaxies, of which 5 are in common with our sample, to look for signatures of young and intermediate massive stars, and they find a frequency of nuclear starburst similar to us.

of young and 40% intermediate age stars. The lowest contributions are found in IC 3639, with fractions of 20% and 40% of young and intermediate age stars, respectively. Because massive stars are very blue and emit most of their flux at ultraviolet and far-ultraviolet wavelengths, the corresponding fractions of young stars will increase to shorter wavelengths. Thus, the ultraviolet spectrum of these nuclei will be dominated by the massive stars, even in the nuclei with a relatively low contribution of young stars to the optical light (as our HST-UV observations of IC 3639 show - GD98).

The contribution of young and intermediate age stars at optical wavelengths in these nuclei are also very similar to the situation in normal starburst nuclei. A prototypical nuclear starburst galaxy is NGC 7714 (Weedman et al. 1981). Its ultraviolet spectrum and nebular optical emission lines are very well explained by a 4-5 Myr old burst (González Delgado et al. 1999). In contrast, its optical continuum shows an important contribution of intermediate age stars. A fit of its ultraviolet to near-infrared spectral energy distribution shows that half of the optical light in the central 2×2 arcsec is provided by a ∼200 Myr burst (Goldader et al. 2000). The near-ultraviolet spectrum of NGC 7714, just like half of the Seyfert 2 nuclei in our sample, shows the higher order terms of the Balmer series in absorption (González Delgado 2000). The strength of these lines are well fitted by two bursts, of 5 and 200 Myr, that contribute to the total light at 4400 Å with a similar fraction as in the cases of NGC 5135 and NGC 7130. The older burst in NGC 7714 could be a consequence of the interaction with its companion, NGC 7715, because the dynamical time scale of the interaction is ∼ few×100 Myr (González Delgado et al. 1995).

From our comparison with NGC 7714, we conclude that half of the S2 of our sample show spectral characteristics that are very similar to prototypical starburst nuclei. On the other hand, the fact that 6 of the 9 S2 nuclei of the sample that show starburst characteristics are interacting or merging systems, suggests that the ∼ few×100 Myr burst could be triggered by the close passage of a companion, such as the merger models of Mihos & Hernquist (1996) predict. According to these and other models (e.g. Athanasoula 1992) based on the existence of a non-axisymmetric potential, the gas sinks toward the central part of the galaxy. There, it could be compressed producing a starburst and feeding the active nucleus.

Young and intermediate age stars have been detected in the optical continuum of other active galaxies. Schmitt et al. (1999) find that the optical light of 30% of the nuclei in a sample of 20 S2 galaxies is dominated by young and intermediate age stars, and 80% of the nuclei have also a significant contribution of 1 Gyr old stars. These stars contribute to the optical light with larger fractions that they do in normal early type galaxies. Intermediate age stars have been found also in the nearby radio galaxy 3C 321 (Tadhunter, Dickinson & Shaw 1996), and in high redshift radio galaxies selected to be very strong far-infrared and radio emitters (Tran et al 1999). The most spectacular case is found in the QSO UNJ1025-0040 (Brotherton et al 1999). Its ultraviolet spectrum shows broad MgII λ2800, while in the near-ultraviolet a strong Balmer absorption series is detected. This QSO could be interacting and the companion galaxy shows also strong Balmer absorption series (Canalizo et al 2000).

Our results and those reported by other groups are pointing to a causal link between the starburst and the Seyfert phenomenon. In this case, the few×100 Myr star formation time scale should be comparable to the duration of the nuclear activity. As Storchi-Bergmann et al (1998) have pointed out, this timescale - $\sim 1\%$ of the Hubble time - would imply that $\sim 1\%$ of the galaxies should be strongly active, as current estimates indicate (e.g. Huchra & Burg 1992).

6.3. Are there two kinds of Seyfert 2's?

The results of the previous sections show that the nuclear and circumnuclear regions of S2 have a variety of stellar population properties. However, most of the nuclei of our sample can be grouped in two classes, those with young and intermediate age stars and those with an optical continuum dominated by old stars. This segregation in two groups poses an important question: are there two different classes of S2 nuclei? That is, do all S2 nuclei contain a hidden S1 nucleus? Do all S2 nuclei contain nuclear starbursts, but undetectably faint in half the cases due to low relative luminosity? We note in this vein that the significantly higher far-IR luminosities of S2 nuclei with young and intermediate age stars (see above) probably rules out a model in which the old-star-dominated S2 nuclei have equally powerful (but more heavily extincted) starbursts.

We can begin to address the above questions by quantifying the relative energetic importance of young stars and the hidden S1 nucleus in our sample. This cannot be done rigorously, but there are some useful empirical diagnostics. The ratio of the mid- and far-IR luminosity should probe the ratio of the S1 and starburst luminosities. Dust-reprocessed radiation from the S1 nucleus peaks in brightness in the mid-IR (cf. Elvis et al. 1994), while starbursts peak in brightness in the far-IR. Optical emission-line diagnostics are also potentially useful. The characteristic excitation state of gas photoionized by the hidden S1 nucleus is very high (e.g. [OIII]λ5007/H$\beta \sim 10$), while starbursts in the nuclei of spiral galaxies have much lower excitation ([OIII]λ5007/H$\beta \leq 1$). Thus, the [OIII]λ5007/Hβ ratio should contain information about the sources of ionizing photons in the S2 nuclei.

Inspection of the infrared colors and excitation indicates that the two S2 groups do indeed have different properties. The excitation measured by [OIII]/Hβ is almost a factor two lower in nuclei with young and intermediate age stars (mean value log([OIII]/Hβ = 0.78±0.07) than in nuclei with an old stellar population (mean value of 0.97±0.06). A similar result is found for the infrared color $f_{25\mu}/f_{60\mu}$. Nuclei with young and intermediate age stars are cooler (mean value of $\log(f_{25\mu}/f_{60\mu})$ = -0.70±0.07) than nuclei with an old stellar population (mean value of -0.40±0.09). These two quantities seem to be related: objects with higher excitation are those with warmer colors (Figure 21). This is as expected if hot (young) stars make a significant contribution to both heating dust and ionizing gas in some (but not all) S2 nuclei (namely the S2 nuclei in which our spectra reveal a substantial young/intermediate age population).

An alternative interpretation of the mid/far-IR ratio in S2 nuclei is suggested by the results of Heisler, Lumsden & Bailey (1997). They found that the probability of detecting scattered broad emission lines from a hidden S1 nucleus is highest in S2 nuclei that have warm infrared colors ($f_{25}/f_{60} > 0.25$) and smaller extinction. According to the unified scheme, S2 nuclei are those in which the molecular torus that surrounds the central source is oriented with its equatorial plane near our line-of-sight. However, there should be S2 nuclei in which the torus is oriented at intermediate angles between the equatorial plane and polar axis. In these nuclei the S1's hidden Broad Line Region (HBLR) will be easily detected in polarized light. At this orientation we are seeing the inner part of the torus that is illuminated directly by the central source. Because the temperature of the dust will be higher in the inner than in the outer parts of the torus, the nuclei with intermediate orientation will be warmer at infrared wavelengths than nuclei oriented with the polar axis perpendicular to us. These results, together with the segregation of the nuclei of our sample in terms of stellar population, excitation, and far-infrared colors, suggests a possible connection between the detection of a HBLRs and the starburst activity in the nuclei of S2.

Most (18 of 20) of the S2 nuclei of our sample have been observed spectropolarimetrically at optical wavelengths (Kay 1994; Tran 1995a; Heisler et al 1997). They show an average optical continuum polarization of a few percent (mean $\sim$ 2%), which is much lower than the degree of polarization expected by the unified scheme unless the continuum is primarily of some other origin (e.g. starlight). The exception is NGC 1068, in which the continuum is polarized by $\sim 16\%$ (Antonucci & Miller 1985). Balmer broad emission lines have been detected in 8 of the nuclei in our sample (Mrk 3, Mrk 348, Mrk 463E, Mrk 477, Mrk 533, NGC 1068, NGC 7212, and IC 3639, Tran 1995abc; Heisler et al 1997), and broad Hβ is also marginally detected in Mrk 573 (Kay 1994). Heisler et al (1997) have also reported the non-detection of HBLRs in two of our nuclei, NGC 5135 and NGC 7130. For the remaining objects, we have not found any information in this respect in the literature. An inspection of Figure 21 indicates that all S2 nuclei of our sample with HBLRs have IR colors warmer than 0.25.

It is important to emphasize that HBLRs are present in at least 3 of the 9 S2 nuclei in our sample with a young/intermediate age stellar population (Mrk 477, Mrk 533, and IC 3639). This compares to 3 of the 8 S2 nuclei dominated by old stars (Mrk 3, Mrk 348, and NGC 7212). This comparison suggests that there is no strong anti-correlation between the presence of a hidden S1 nucleus and a nuclear starburst. This is at odds with a model in which one class of S2 nuclei are powered by hidden S1 nuclei and another class is powered by a nuclear starburst.

Our HST ultraviolet observations of Mrk 477, NGC 5135, NGC 7130 and IC 3639 have shown that the starbursts in these S2 nuclei are very powerful, dusty and compact. They have sizes that are similar to the NLR, and they are also similar to the torus sizes reported through detections at near-IR and millimeter wavelengths (Young et al 1996; Tacconi et al 1994). This similarity in the sizes suggests that these starbursts may be formed at the outskirts of the molecular torus. This is a natural location where the star formation can be triggered, because the torus may serve as a reservoir of molecular gas at a few hundred parsecs from the nucleus. Thus, if the obscuring torus is a basic component of the Seyfert phenomenon, nuclear starbursts should be ubiquitous in S2 nuclei.

If this is the case, why don't we see starbursts in all S2 nuclei? One possibility is that more sensitive spectroscopy (perhaps at the much higher spatial resolution of HST+STIS) would reveal compact but inconspicuous starbursts in the S2 nuclei whose ground-based spectra are dominated by the light of old stars on the few-arcsec-scale. Alternatively, perhaps the obscuring torus sustains intermittent bursts of star-formation with a duty cycle of roughly 50%. The results reported by GD98 are consistent with this picture, since they found that the stellar population in four well-studied S2 nuclei was consistent with short-lived bursts with durations of only a few Myr. On the other hand, such a picture would be inconsistent with the absence of a significant intermediate age stellar population in roughly half our S2 sample (those whose light is dominated by old stars).

6.4. The nature of the blue continuum: breaking the young star versus power law degeneracy

In order to know the nature of the FC in Seyfert nuclei we need to break the degeneracy between power-law and young stars. Our analysis has shown that the blue optical continuum is provided by a nuclear starburst that dominates the near-ultraviolet light in about half of the S2 in the sample. In these nuclei, the degeneracy between power-law and young stars is completely broken because the blue continuum at the near-ultraviolet is not feature-less at all; on the contrary, it is dominated by absorption features (HOBS and HeI lines) formed in the photosphere of young stars. Thus, the photospheric HOBS and HeI are a powerful diagnostic to discriminate between a blue continuum povided by a young and intermediate age population or by scattered light from a hidden S1. G-band and CaII H and K lines cannot help to break the degeneracy because these lines can be diluted in the same way by young stars or by a scattered light.

However, if the starburst is in a nebular phase (younger than about a few Myr), Balmer absorption lines cannot help much to break the degeneracy. The stellar lines (the equivalent widths of the HOBL is less of 3 Å) are filled by the nebular emission provided by this young starburst (see figure 16 in González Delgado, Leitherer & Heckamn 1999). HeI λ3819, 4026 and 4388 lines may be a better diagnostic since after 4-5 Myr, this HeI nebular emission provided by the starburst drop and the stellar absorption dominates. In practice, it is difficult to break the degeneracy with HeI lines because these are weaker and they may be also filled by the NLR contribution. The detection of WR features, as in the case Mrk 477, may also help to break the degeneracy. The equivalent width of the Balmer emission cannot be a good diagnostic because the NLR can also contribute to the nebular emission, and the bulge stellar population can contribute to the optical continuum, and differential extinction can affect unevenly gas and stars. Of course, in Seyfert nuclei with very young starbursts, the degeneracy is totally broken in the ultraviolet because O stars are very rich in wind resonance lines (CIV, SiIV, NV, etc).

7. Summary and conclusions

Our most important conclusions from the near-ultraviolet and optical observations of 20 of the brightest known Seyfert 2 nuclei are as follows:

- In 8 of the nuclei (Mrk 3, Mrk 34, Mrk 348, Mrk 573, NGC 1386, NGC 2110, NGC 5929 and NGC 7212) the stellar lines are similar to those of an old population. The presence of scattered light produced by the hidden nucleus is required to fit the spectra in only four of them, Mrk 3, Mrk 34, Mrk 573 and NGC 7212. However, only Mrk 3 shows a significant dilution of the stellar lines in its nucleus compared to its circumnuclear region. The lack of extra dilution in the nuclei of Mrk 34, Mrk 573, and NGC 7212 suggests the presence of a spatially-extended “featureless” continuum.

- The spectral energy distribution and the strength of the stellar lines in the nuclei and circumnuclear regions of Mrk 78 and NGC 1068 require a significant contribution of an intermediate age population in addition to the old bulge component. However, 10% and 15% (respectively) of the total optical light could also be due to scattered light from their hidden Seyfert 1 nuclei. In the case of NGC 1068, the result is in agreement with the fact that its optical continuum is highly polarized.

- Six of the nuclei (Mrk 273, Mrk 1066, Mrk 1073, NGC 5135, NGC 7130 and IC 3639) show HeI and/or strong Balmer absorption lines in the near-ultraviolet. Three other galaxies (Mrk 1, Mrk 477 and Mrk 533) show the higher order terms of the Balmer series in absorption in their circumnuclear regions, and in their nuclear spectra when the nebular emission contributions are subtracted. Mrk 463E may be a similar object, but better data are needed to confirm this. The analysis of the stellar lines using evolutionary synthesis models suggests that the dominant stellar population in these nuclei consists of young and intermediate age stars. These galaxies show a significant dilution of the lines in their nuclei compared to their circumnuclear regions. Thus, hot (young) stars are more conspicuous in the nucleus than in the bulge or inner disk.

- A broad emission feature centered at around 4680 Å is present in three nuclei in our sample: Mrk 1, Mrk 463E, and Mrk 477. It is most plausibly ascribed to a population of Wolf Rayet stars (cf. H97), but confirmation will require the detection of other signatures of Wolf Rayet stars.

- Comparison with the prototypical starburst nucleus in NGC 7714 indicates that roughly half of the Seyfert 2 nuclei in our sample show characteristics that are very similar to starburst nuclei. Therefore, it is expected that young massive stars will dominate the ultraviolet spectra of these nuclei. This has been directly confirmed for four members of our sample (H97, GD98).

- The nuclei with young and intermediate-age populations show lower excitation (smaller [OIII]/Hβ flux ratio), larger far-IR luminosities, and cooler $f_{25\mu}/f_{60\mu}$ IRAS colors than nuclei dominated by an old stellar population. These differences are as expected if a starburst makes a substantial contribution to the heating of the dust and the ionization of the gas in the former set of nuclei, but not the latter.
- The fact that hidden BLRs have been found in nuclei with young and intermediate-age stars (Mrk 477, Mrk 533 and IC 3639) implies that the presence of starbursts and hidden Seyfert 1 nuclei are not anti-correlated. That is, there is no evidence for two distinct types of Seyfert 2 nuclei (starburst-powered and AGN-powered).

Acknowledgments

We are grateful to Enrique Pérez and Luis Colina for many stimulating discussions and helpful suggestions, and to the staff at KPNO for their help in obtaining the data presented in this paper. This work was supported by Spanish DGICYT projects PB98-0521, by the NASA LTSA grant NAG5-6400, and by HST grants GO-5944 and GO-6539 from the Space Telescope Science Institute, which is operated by the Association of Universities for Research in Astronomy, Inc., under NASA contract NAS5-26555.

REFERENCES

Antonucci, R.R.J., & Miller, J.S. 1985, ApJ, 297, 621

Athanassoula, R. 1992, MNRAS, 259, 345

Bica, E., Alloin, D., & Schmidt, A.A. 1990, A&A, 228, 23

Bica, E., Santos, J.F.C., & Alloin, D. 1990, A&A, 235, 103

Bonatto, C.J., & Pastoriza, M.G. 1997, ApJ, 486, 132

Brotherton, M.S., van Breugel, W., Stanford, S.A., Smith, R.J., Boyle, B.J., Miller, L., Shanks, T., Croom, S,M., Filippenko, A.V., 1999, ApJ, 520, 87

Calzetti, D., Kinney, A.L., & Storchi-Bergmann, T. 1994, 429, 582

Canalizo, G., Stockton, A., Brotherton, M.S., & van Breugel, W. 2000, AJ, 119, 59

Cid Fernandes, R., Terlevich, R. 1995, MNRAS, 272, 423

Cid Fernandes, R., Storchi-Bergmann, T., & Schmitt, H.R. 1998, MNRAS, 297, 579

De Robertis, M. 1987, ApJ, 316, 597

Díaz, A.I., Terlevich, E. & Terlevich, R. 1989, MNRAS, 239, 325

Elvis, M., Wilkes, B.J., McDowell, J.C., Green, R.F., Bechtold, J., Willner, S.P., Oey, M.S., Polomski, E. & Cutri, R. 1994, ApJS, 95, 1

Filippenko, A.V. & Terlevich, R. 1992, ApJ, 397, L79

García-Vargas, M.L., Mollá, M., & Bressan, A. 1998, A&AS, 130, 513

Goldader, J. et al. 2000, in preparation

González Delgado, R.M. 2000, New Astronomy Review, in press

González Delgado, R.M., Pérez, E., Díaz, A., García-Vargas, M.L., Terlevich, E., Vílchez, J.M. 1995, ApJ, 439, 604

González Delgado, R.M. & Pérez, E. 1996, MNRAS, 281, 781

González Delgado, R.M., Leitherer, C., Heckman, T., & Cerviño, M. 1997, 483, 705

González Delgado, R.M., Leitherer, C., Heckman, T., Lowenthal, J., Feguson, H., & Robert, C. 1998a, ApJ, 495, 698

González Delgado, R.M., Heckman, T. Leitherer, C., Meurer, G., Krolik, J., Wilson, A.S., Kinney, A. & Koratkar, A. 1998b, ApJ, 505, 174

González Delgado, R.M., García-Vargas, M.L., Goldader, J., Leitherer, C., Pasquali, A. 1999, ApJ, 513, 707

González Delgado, R.M., & Leitherer, C. 1999, ApJS, 125, 479

González Delgado, R.M., Leitherer, C., & Heckman, T. 1999, ApJS, 125, 489

González Delgado, R.M. & Pérez, E. 2000, MNRAS, in press

Heckman, T.M. 1996, in *The Physics of Liners in View of Recent Observations*, eds. M. Eracleous, A. Koratkar, C. Leitherer & L. Ho, ASP-CS 103, 241

Heckman, T.M., González-Delgado, R., Leitherer, C., Meurer, G.R., Krolik, J., Kinney, A., Koratkar, A., & Wilson, A.S. 1997, ApJ, 482, 114

Heckman, T.M., Krolik, J., Meurer, G., Calzetti, D., Kinney, A., Koratkar, C., Leitherer, C., & Robert, C. 1995, ApJ, 452, 549

Heisler, C.A., Lumsden, S.L., & Bailey, J.A. 1997, Nature, 385, 700

Ho, L.C., Filippenko, A.V., & Sargent, W.L. 1995, ApJS, 98, 477

Huchra, J., & Burg, R. 1992, ApJ, 393, 90

Kay, L. 1994, ApJ, 430, 196

Kunth, D. & Contini, T. 1999, in *Wolf-Rayet phenomena in massive stars and starburst galaxies*, eds. Van der Hucht, K.A., Koenigsberger, G. & Eenens, P.R.J., IAU Symposium 193, 725

Maoz, D., Koratkar, A., Shields, J., Ho, L., Filippenko, A.V., Sternberg, A. 1998, AJ, 116, 55

Mayya, Y.D., 1997, ApJ, 482, 149

Meurer, G., Heckman, T.M., Leitherer, C., Kinney, A., Robert, C., & Garnett, D. 1995, AJ, 110, 2665

Mihos, J.C., & Hernquist, L. 1996, ApJ, 464, 641

Nelson, C., & Whittle, M. 1995, ApJSS, 99, 67

Schmitt, H.R., Storchi-Bergmann, T., & Cid Fernandes, R., 1999, MNRAS, 303, 173

Storchi-Bergmann, T.,Raimann, D., Bica, E.L.D., Fraquelli, H.A. 2000, ApJ, accepted

Storchi-Bergmann, T., Cid Fernandes, R., & Schmitt, H.R. 1998, ApJ, 501, 94

Storchi-Bergmann, T., Scmitt, H.R., Calzetti, D., Kinney, A.L. 1998, AJ, 115, 909

Storchi-Bergmann, T., Kinney, A., & Challis, P. 1995, ApJ, 98, 103

Tacconi, L.J., Genzel, R., Blietz, M., Cameron, M., Harris, A.I., & Madden, S. 1994, ApJ, 426, L77

Tadhunter, C.N., Dickson, R.C. & Shaw, N.A. 1996, MNRAS, 281, 591

Terlevich, E., Díaz, A.I., & Terlevich, R. 1990, MNRAS, 242, 271

Tran, H.D. 1995a, ApJ, 440, 565

Tran, H.D. 1995b, ApJ, 440, 578

Tran, H.D. 1995c, ApJ, 440, 597

Tran, H.D., Brotherton, M.S., Stanford, S.A., van Breugel, W., Dey, A., Stern, D., & Antonucci, R. 1999, ApJ, 516, 85

Weedman, D.W., Feldman, F.R., Balzano, V.A., Ramsey, L.W., Sramek, R.A., Wu, C.-C. 1981, ApJ, 248, 105

Whittle, M. 1992a, ApJ, 387, 121

- -, 1992b, ApJS, 79, 49

Walborn, N.R., & Fitzpatrick, E.L. 1990, PASP, 102, 379

Wilkins, T.N. & Axon, D.J., 1991, TWODSPEC, Starlink User Note, No. 16.

Young, S., Packham, C., Hough, J.H., & Efstathiou, A. 1996, MNRAS, 283, L1

This manuscript was prepared with the AAS LaTeX macros v4.0.

Table 1. Properties of the Seyfert 2 galaxies [a]

Name	Type	v km/s	1 arcsec pc	log $L_{[OIII]}$ erg s^{-1}	log $L_{1.4}$ erg s^{-1}	log L_{12} L⊙	L_{FIR} 10^{10} L⊙	L_{IR} 10^{11} L⊙
Mrk 1	S	4780	310	41.62	38.69	10.77	1.5	0.9
Mrk 3	S0:	4050	260	42.28	39.78	10.20	1.5	0.6
Mrk 34	S:	15150	980	42.68	39.09	10.33	4.6	1.4
Mrk 78	SB	11145	720	42.39	39.11	10.34	3.6	1.1
Mrk 273	Ring Gal. pec	11334	730	41.97	39.73	10.61	71.0	12.0
Mrk 348	SA(s)0/a:	4540	290	41.46	39.39	10.15	0.7	0.3
Mrk 463E	S pec	14904	960	42.70	40.46	11.19	11.7	5.0
Mrk 477	S	11340	730	42.79	39.40	10.34	5.5	1.5
Mrk 533	SA(r)bc pec	8713	563	42.03	39.70	10.85	11.9	3.1
Mrk 573	SAB(rs)0+:	5174	335	42.07	38.03	9.96	0.8	0.3
Mrk 1066	SB(s)0+	3605	235	40.97	38.58	9.90	3.6	0.6
Mrk 1073	SB(s)b	6991	450	41.50	39.35	10.47	10.9	2.2
NGC 1068	SA(rs)b	1136	75	41.88	39.17	10.85	6.1	2.1
NGC 1386	SB(s)0+	924	60	40.64	37.12	8.76	0.1	0.03
NGC 2110	SAB0-	2284	150	40.44	38.63	9.40	0.6	0.1
NGC 5135	SBab	4112	270	41.05	38.93	10.17	3.9	0.9
NGC 5929	Sab:pec	2753	180	40.40	38.36	9.65	2.0	0.4
NGC 7130	Sa pec	4842	310	41.28	38.99	10.28	11.1	2.0
NGC 7212	S	7994	515	42.09	–	10.23	5.5	1.2
IC 3639	SBbc	3285	210	40.77	38.47	10.00	2.3	0.5

[a] Data for the [OIII] λ5007+4959 and 1.4 GHz radio continuum are from Whittle (1992b). The FIR luminosity was computed from the 60 and 100 μm IRAS fluxes (Fullmer & Lonsdale 1989); and IR luminosity was computed using all 4 IRAS fluxes (Sanders & Mirabel 1997). Radial velocities and morphological type are from NED. H_0=75 km s^{-1} Mpc^{-1}

Table 2. Log of the Observations

Name	Date	Exp. Time s	P.A. degree	Air mass	Date	Exp. Time s	P.A. degree	Air mass
Mrk 1	Oct 11	2×1200	95	1.02	Oct 11	2×1800	95	1.0
Mrk 3	Feb 16	1200, 600	164	1.3	Feb 15	2×1800	144	1.3
Mrk 34	Feb 16	900, 1200	37	1.16	Feb 14	2×1800	162	1.15
Mrk 78	Feb 16	2×900	165	1.2	Feb 15	2×1800	160	1.2
Mrk 273	Feb 16	900,1200	73	1.3	Feb 15	3×1800	70	1.2
Mrk 348	Oct 10	2×1200	98	1.0	Oct 11	2×1800	98	1.05
Mrk 463E	Feb 16	900,600	160	1.0	Feb 14	2×1800	175,134	1.05
Mrk 477	Feb 16	2×1200	144,158	1.0	Feb 14	1800,900	0	1.1
Mrk 533	Oct 10	2×1200	162	1.1	–	–	–	–
Mrk 573	Oct 10	2×1200	161	1.15	Oct 11	2×1800	161	1.2
Mrk 1066	Oct 10	2×1200	96	1.1	Oct 11	1800,900	96	1.1
Mrk 1073	Oct 10	1200,900	96	1.2	Oct 11	1800,900	96	1.2
NGC 1068	Oct 10	900,600,300	123	1.2	Oct 11	2×900	123	1.2
NGC 1386	Oct 10	2×1200	360	2.6	Oct 11	2×1200	0	2.6
NGC 2110	Feb 16	2×900	6	1.3	Feb 15	1800	5	1.3
NGC 5135	Feb 16	2×900	173	2.1	–	–	–	–
NGC 5929	Feb 16	2×900	60,80	1.03	Feb 15	1800,900	80	1.1
NGC 7130	Oct 10	1200,1800	177	2.55	Oct 11	1800	177	2.55
NGC7212	Oct 10	2×1200	136	1.15	Oct 11	2×1800	136	1.1
IC 3639	Feb 16	2×1200	170	2.7	–	–	–	–
NGC 205	Feb 16	300,2×600	82	1.6	Feb 15	300,2×600	85	1.55
NGC 1569	Feb 16	2×600	140	1.2	Feb 14	2×600	140	1.2
NGC 4339	Feb 16	600,900	130	1.35	Feb 15	300,2×600	135	1.2

Table 3. Equivalent widths (in Å units) of the Hβ emission-line and the stellar absorption lines CaII K λ3918, G band and the Calcium triplet at λ8498, λ8542, and λ8662

Name	Hβ emiss	CaII K	G band	CaII λ8498	CaII λ8542	CaII λ8662
Mrk 1	69±3	5.6±0.5	3.1±0.3	1.3±0.3	2.8±0.3	1.9±0.3
Mrk 3	73±3	8±1.3	4.1±0.2	1.4±0.2	2.4±0.2	1.6±0.2
Mrk 34	45±2	8±1.0	4.8±0.4	-	-	-
Mrk 78	12.5±0.5	8.3±0.9	3.9±0.3	1.4±0.1	3.5±0.1	-
Mrk 273	11.4±0.6	5.0±0.5	1.9±0.2	-	2.6±0.3	-
Mrk 348	23.3±0.8	9.5±1.2	5.9±0.5	1.3±0.2	3.2±0.2	3.3±0.2
Mrk 463E	118±6	0.9±0.7	0	-	-	-
Mrk 477	126±5	0.8±0.3	0.6±0.3	-	2.6±0.4	-
Mrk 533	45±1.4	3.8±0.4	1.9±0.3	-	-	-
Mrk 573	22.0±0.9	11±1.5	5.5±0.6	1.3±0.2	3.5±0.2	3.1±0.2
Mrk 1066	25.7±0.6	4.8±0.3	1.8±0.3	1.3±0.1	2.9±0.1	-
Mrk 1073	21.2±0.5	5.0±0.4	2.6±0.3	1.0±0.2	2.7±0.3	-
NGC 1068	39.0±1.3	6.3±0.5	2.7±0.3	1.2±0.1	2.9±0.1	2.6±0.1
NGC 1386	3.2±0.4	12.2±0.8	5.9±0.6	2.2±0.1	3.8±0.1	3.3±0.1
NGC 2110	15.8±0.9	11±1.5	5.6±0.3	1.3±0.1	2.8±0.1	2.1±0.1
NGC 5135	13.8±0.3	3.1±0.2	1.8±0.3	-	-	-
NGC 5929	14.0±0.7	11±1.0	7.1±0.7	1.3±0.2	3.0±0.2	2.2±0.2
NGC 7130	17.4±0.4	3.0±0.2	1.6±0.4	1.3±0.2	3.0±0.2	-
NGC7212	60±3	8.3±0.9	4.3±0.4	1.2±0.6	2.1±0.6	-
IC 3639	18.5±0.7	6.8±0.4	4.1±0.4	-	-	-
NGC 205	-	5.6±0.6	3.9±0.5	1.2±0.2	2.8±0.2	2.4±0.2
NGC 1569B	-	1.8±0.2	1.5±0.2	-	3.7±0.3	3.2±0.1
NGC 4339	-	14±1.4	8±1.1	1.3±0.1	3.6±0.1	3.1±0.1

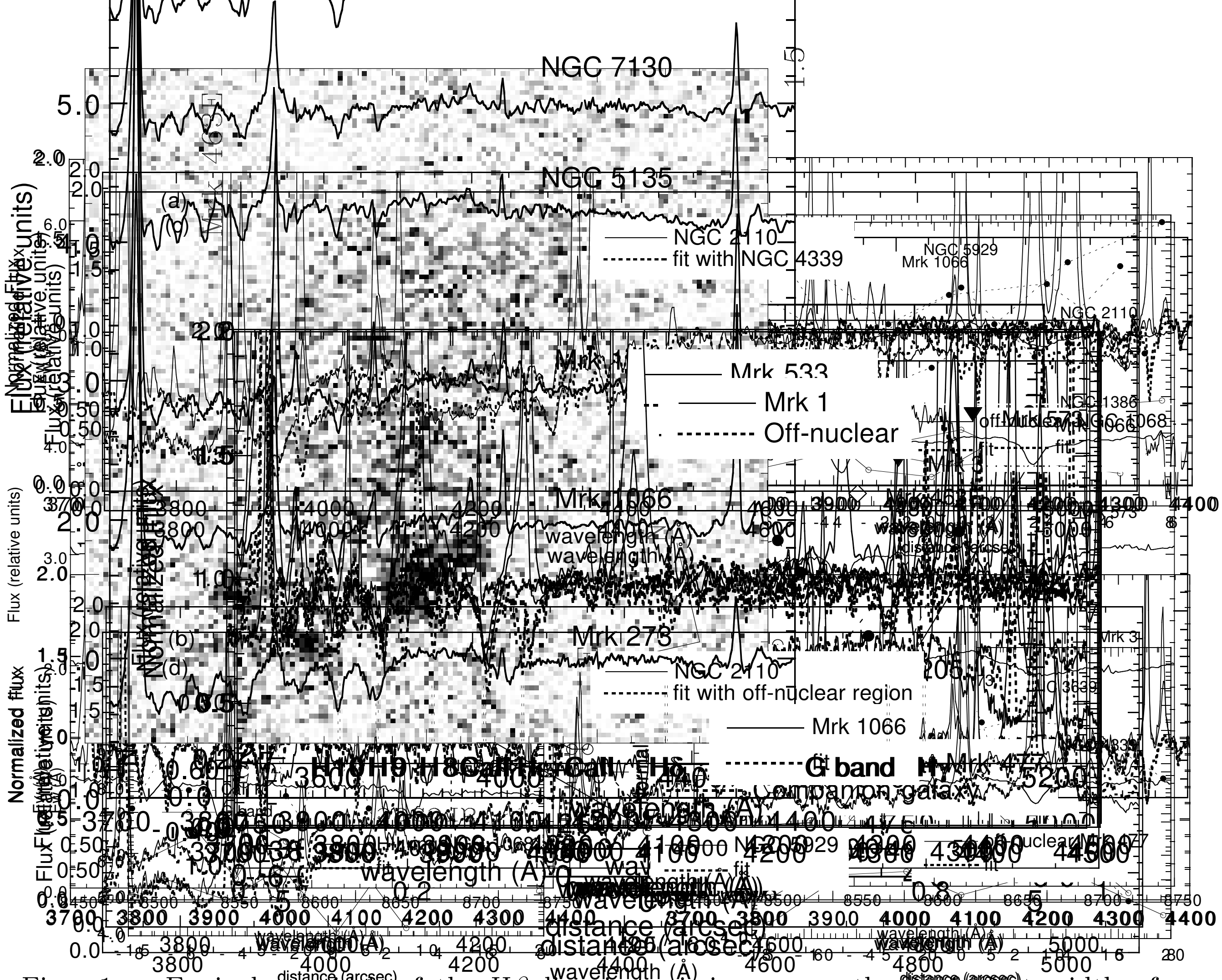

Fig. 1.— Equivalent width of the Hβ line in emission versus the equivalent width of the stellar G band, measured in the nuclear spectra corresponding to a 1.5×2.1 arcsec^2 aperture centered at the peak of the optical continuum at 4550 Å. The different symbols correspond to the four groups in which the objects are classified. Objects with only very weak stellar absorption-lines (Mrk 463E and Mrk 477) are represented by diamonds; those with a continuum dominated by an old stellar population (Mrk 3, Mrk 34, Mrk 348, Mrk 573, NGC 1386, NGC 2110, NGC 5929 and NGC 7212) by triangles; objects with a dominant young and intermediate-age stellar population (Mrk 273, Mrk 1066, Mrk 1073, NGC 5135, NGC 7130, IC 3639, Mrk 1 and Mrk 533) by open circles; and objects in which the stellar population has an important contribution from intermediate-age stars (Mrk 78 and NGC 1068) by filled circles. Dashed lines mark the values of the Ew(G band) of the post-starburst nucleus of NGC 205 (3.6 Å), of the typical elliptical galaxy NGC 4339 (7.6 Å), and of the super-star cluster B in the starburst NGC 1569 (1.5 Å).

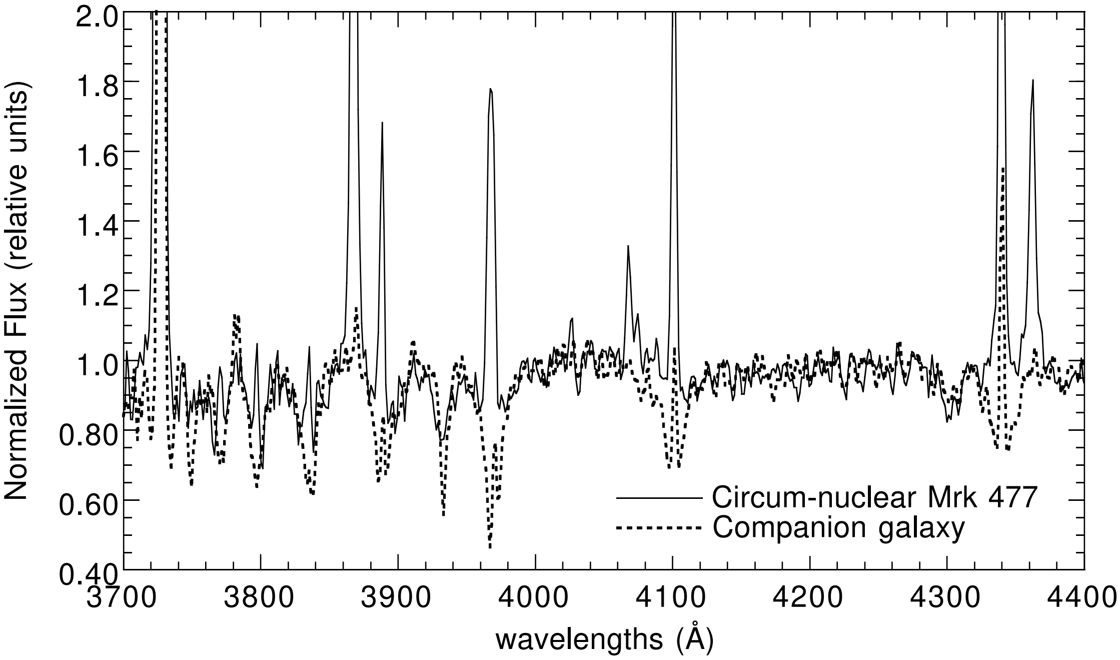

Fig. 2.— Normalized off-nuclear spectrum of Mrk 477 obtained through a 1.5×2 arcsec^2 aperture at 2 arcsec from the optical continuum peak. The nuclear spectrum of the companion galaxy of Mrk 477 is shown for comparison (dotted line). Both show the higher order terms of the Balmer series in absorption.

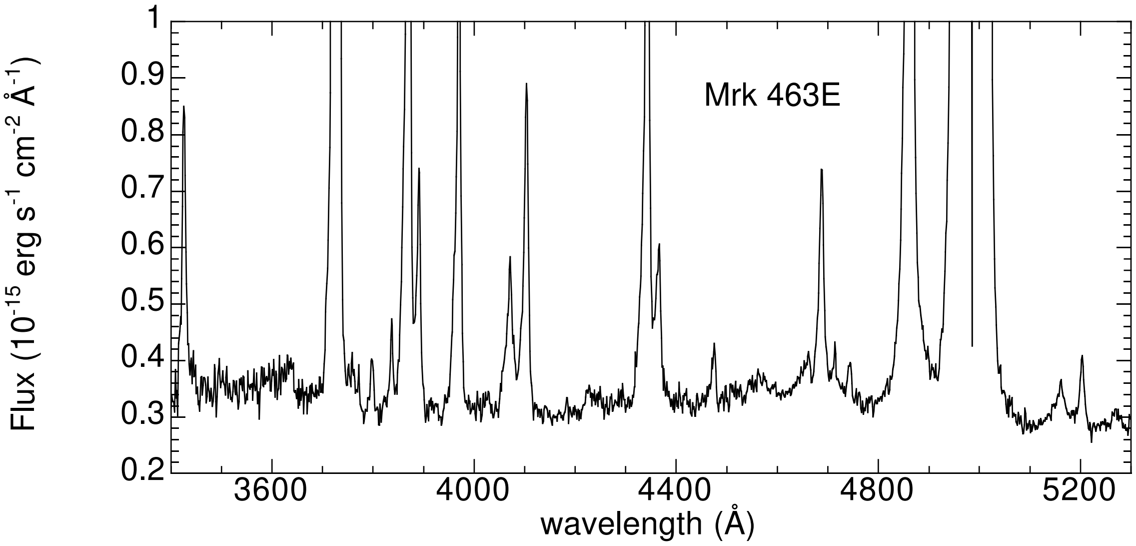

Fig. 3.— Ground-based optical spectrum of Mrk 463E obtained through a 1.5×2.1 arcsec^2 aperture. It shows a broad emission feature at 4680 Å that may be due to a population of Wolf Rayet stars.

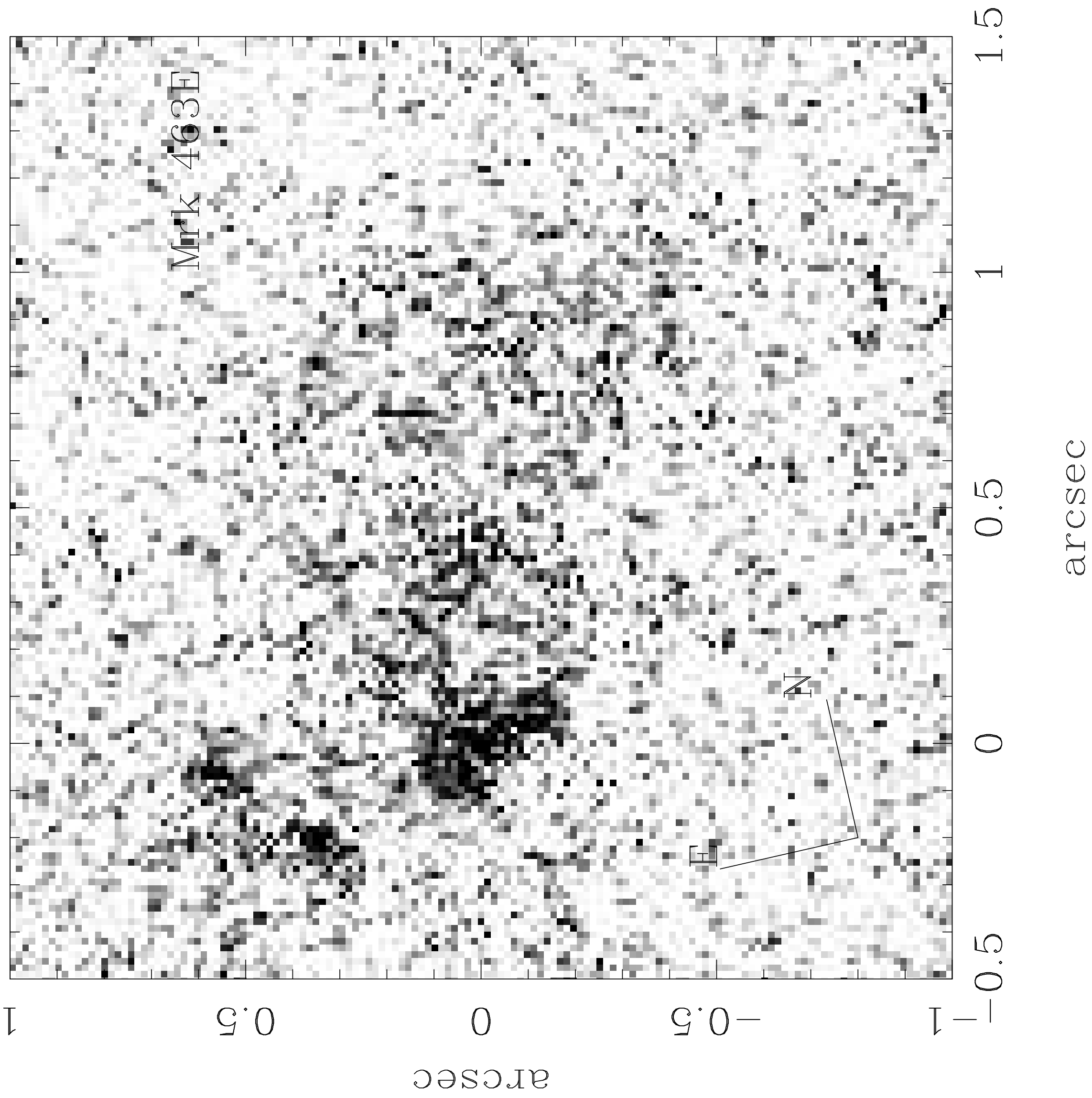

Fig. 4.— *HST*+FOC (through F210M) image of the central 2×2 arcsec^2 (2 by 2 kpc) of Mrk 463E. The morphology is different from the other S2 galaxies that harbor a nuclear starburst. The S2 nucleus is located at the brightest UV knot, whose nature is unknown. Most of the UV flux comes from 1 kpc-scale extended emission.

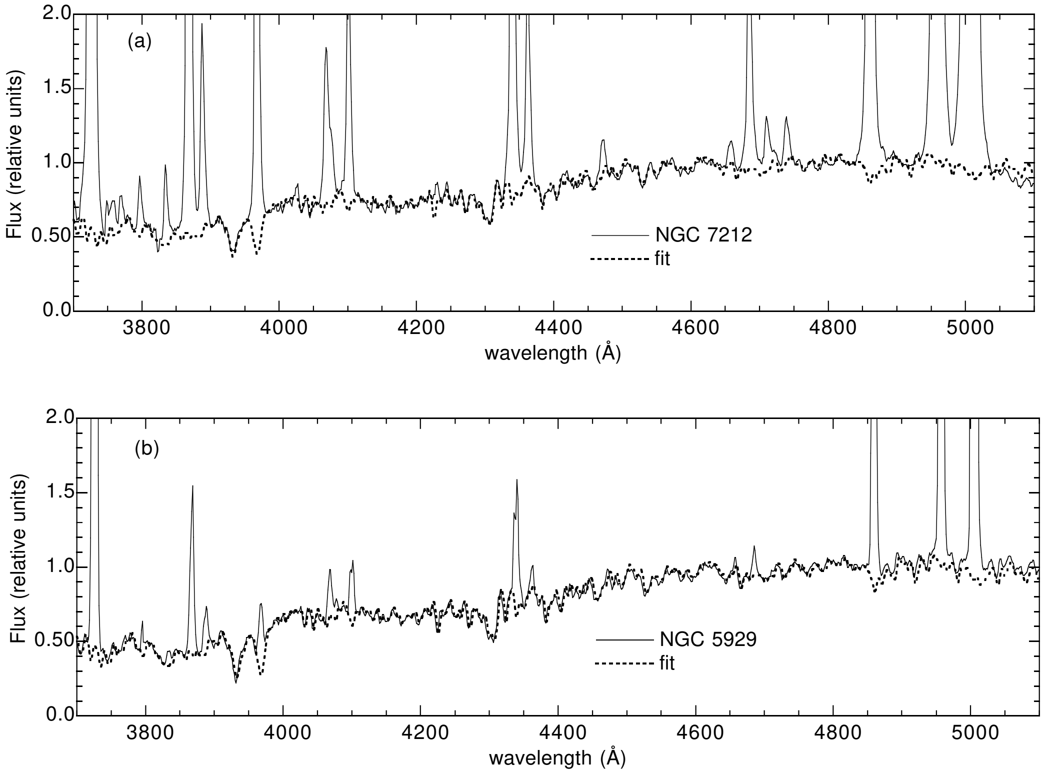
(a)
Flux (relative units)
2.0
1.5
1.0
0.50
0.0
3800
4000
4200
4400
4600
4800
5000
wavelength (Å)
NGC 7212
fit
(b)
Flux (relative units)
2.0
1.5
1.0
0.50
0.0
3800
4000
4200
4400
4600
4800
5000
wavelength (Å)
NGC 5929
fit

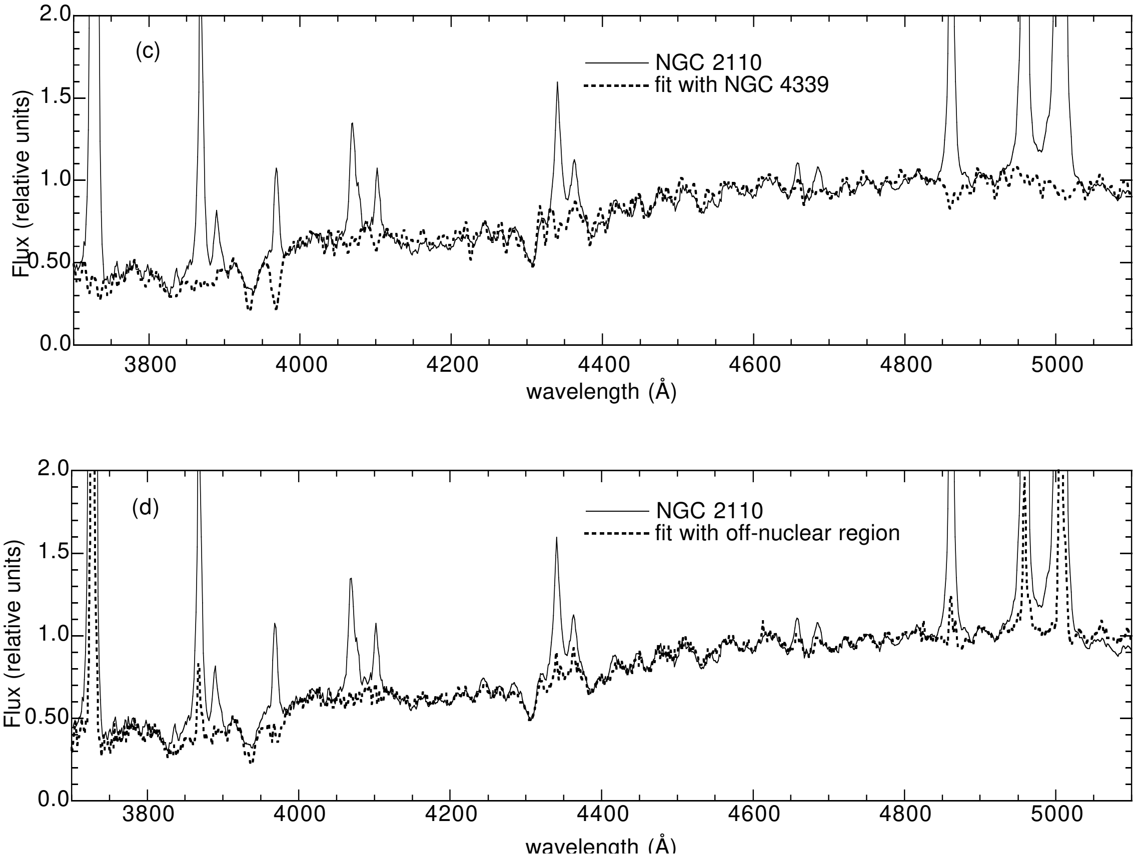

Fig. 5.— Nuclear spectra of three objects NGC 7212 (a), NGC 5929 (b), and NGC 2110 (c and d) that belong to the second group, i.e., nuclei with a stellar population similar to that of elliptical galaxies. Also shown is the best fit to the optical continuum, obtained by combining the elliptical galaxy NGC 4339 plus a power-law (a, b and c). The power-law accounts for 15%, 10% and 5% of the total light at 4800 Å in NGC 7212, NGC 5929 and NGC 2110, respectively. The nebular Balmer continuum is also added to the fit of NGC 7212, contributing 5% of the total light at 4800 Å. Figure 5d shows the result of fitting the nuclear spectrum of NGC 2110 with a circumnuclear spectrum that is reddened by E(B-V)=0.2. This spectrum is the average of two spectra extracted at 5 arcsec from the peak of the optical continuum at 4550 Å. The spectra are all normalized to the flux of the continuum at 4800 Å.

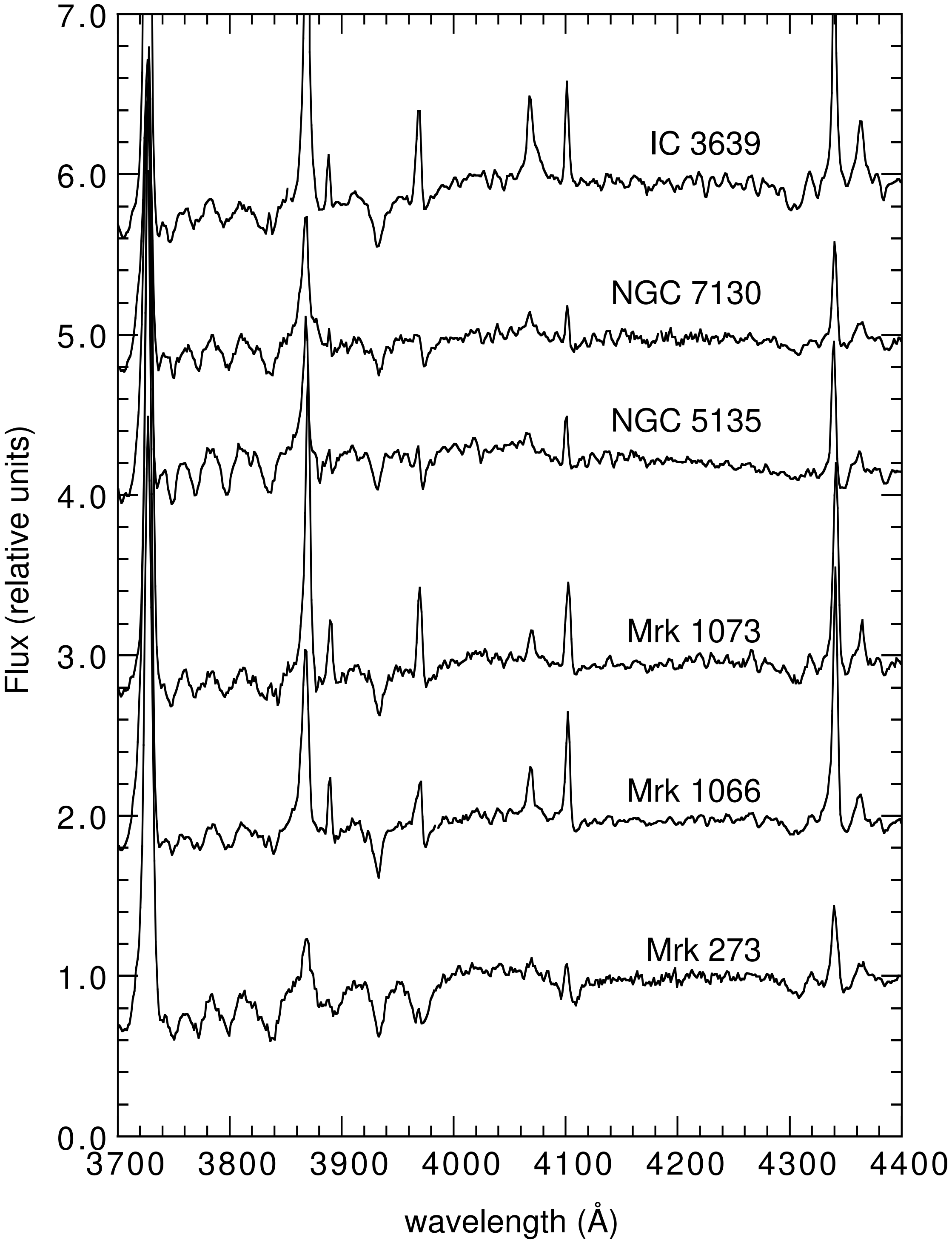

Fig. 6.— Nuclear spectra of objects that show the higher order terms of the Balmer series in absorption (Mrk 273, Mrk 1066, Mrk 1073, NGC 5135, NGC 7130, and IC 3639). All the spectra are normalized to the continuum flux at 4800 Å. They are plotted with an arbitrary offset in flux for clarity.

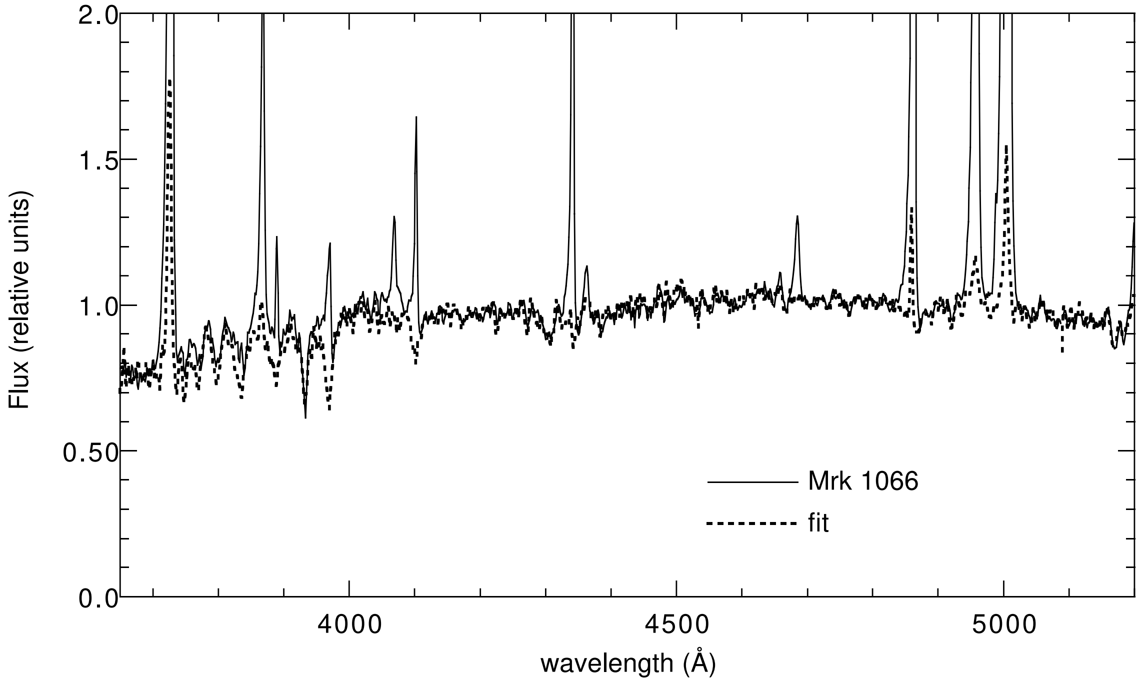

Fig. 7.— The nuclear spectrum of Mrk 1066 normalized to the flux at 4800 Å, and the fit resulting from combining a circumnuclear spectrum plus a power-law that contributes 30% to the total light at 4800 Å (dotted line). The circumnuclear spectrum is extracted at 3.5 arcsec from the optical continuum peak.

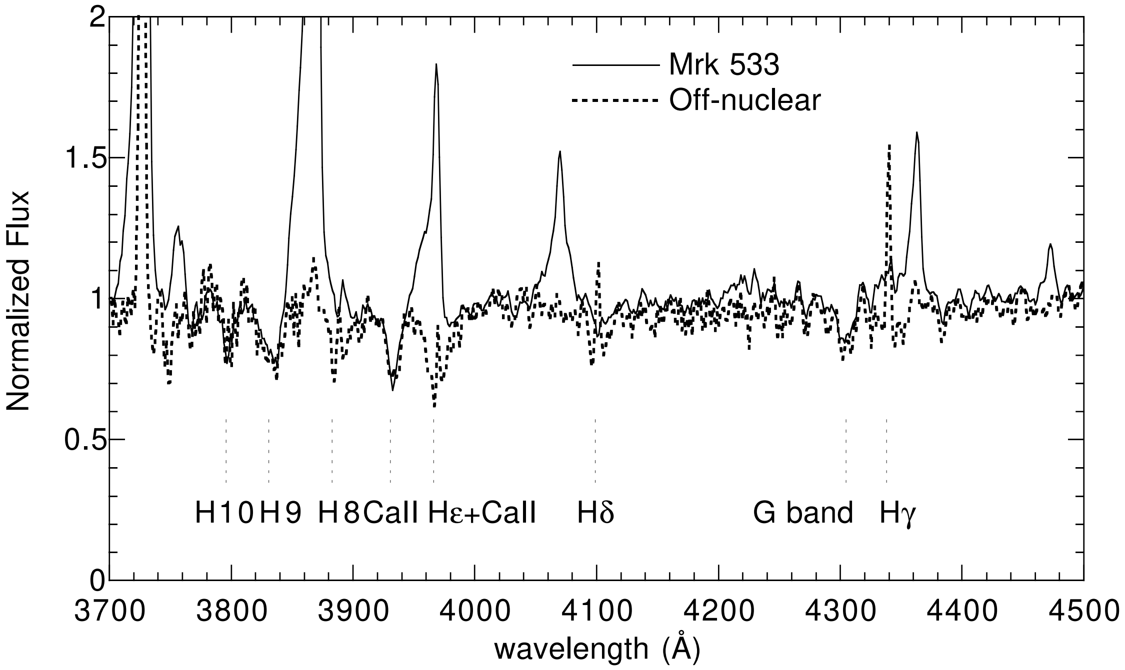

Fig. 8.— The nuclear spectrum of Mrk 533, after the nebular emission of Hδ-H10 is subtracted from the observed spectrum, is compared with an off-nuclear spectrum (dotted line) of Mrk 533 extracted 5 arcsec away from the optical continuum peak. Both show similar Balmer absorption features below 4000 Å.

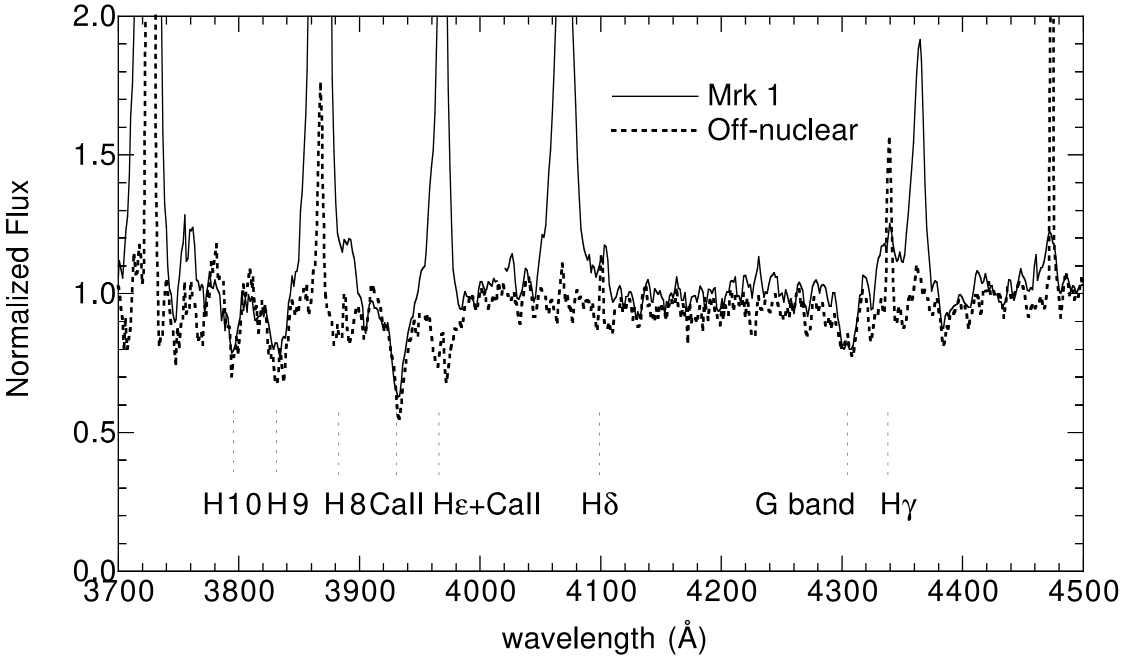

Fig. 9.— As in Figure 8, but for Mrk 1. The circumnuclear spectrum (dotted line) is extracted at 3 arcsec from the optical continuum peak. Both show similar Balmer absorption features below 4000 Å.

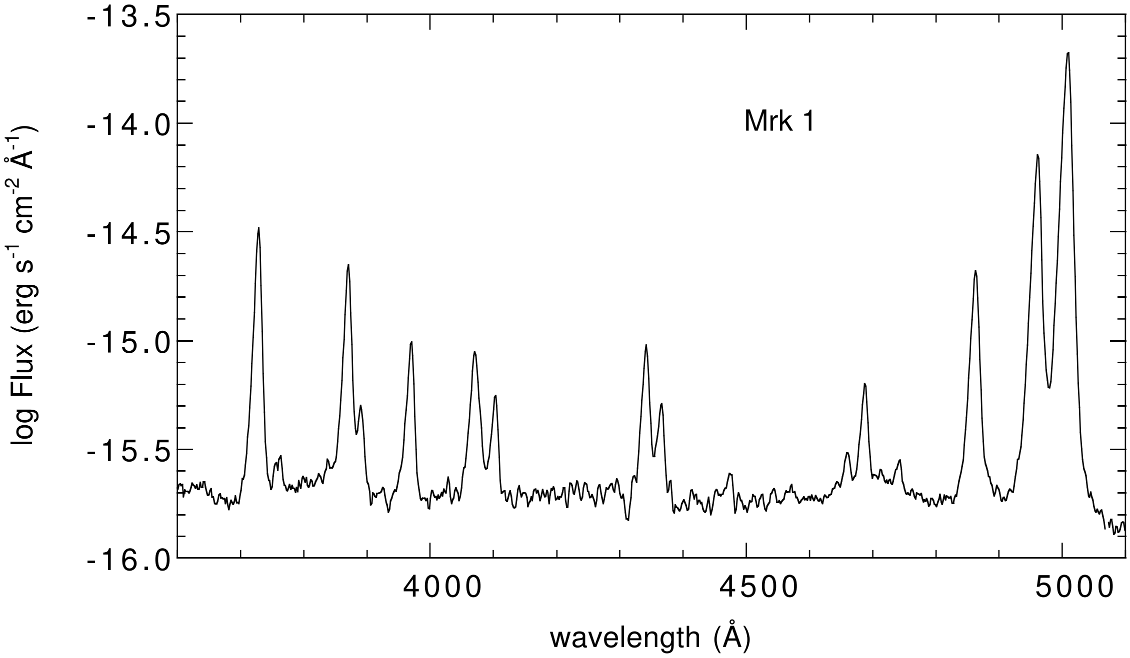

Fig. 10.— Ground-based optical spectrum of Mrk 1 after the absorption-lines due to old stars have been subtracted using the spectrum of a K giant star. It shows a broad emission feature at 4680 Å that may be due to a population of Wolf Rayet stars.

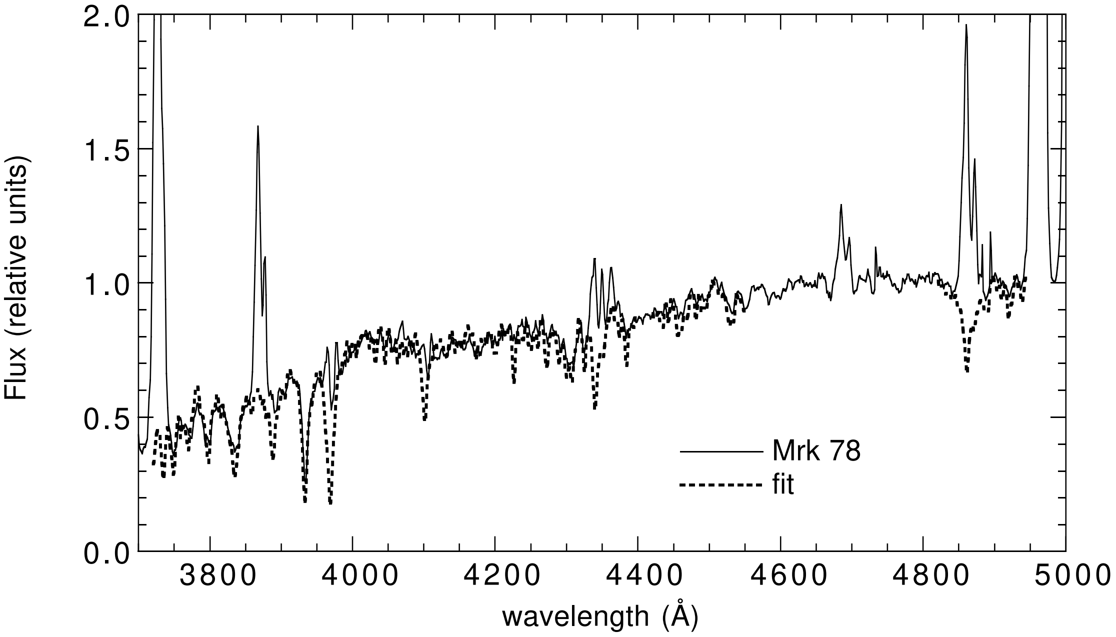

Fig. 11.— Nuclear spectrum of Mrk 78 normalized to the flux at 4800 Å, compared with the result of combining the elliptical galaxy NGC 4339 with the synthetic spectrum predicted by our evolutionary models for a 1 Gyr old instantaneous burst (dotted line). Each component contributes 50% of the total light at 4800 Å. The resulting spectrum fits the stellar features and the continuum spectral energy distribution.

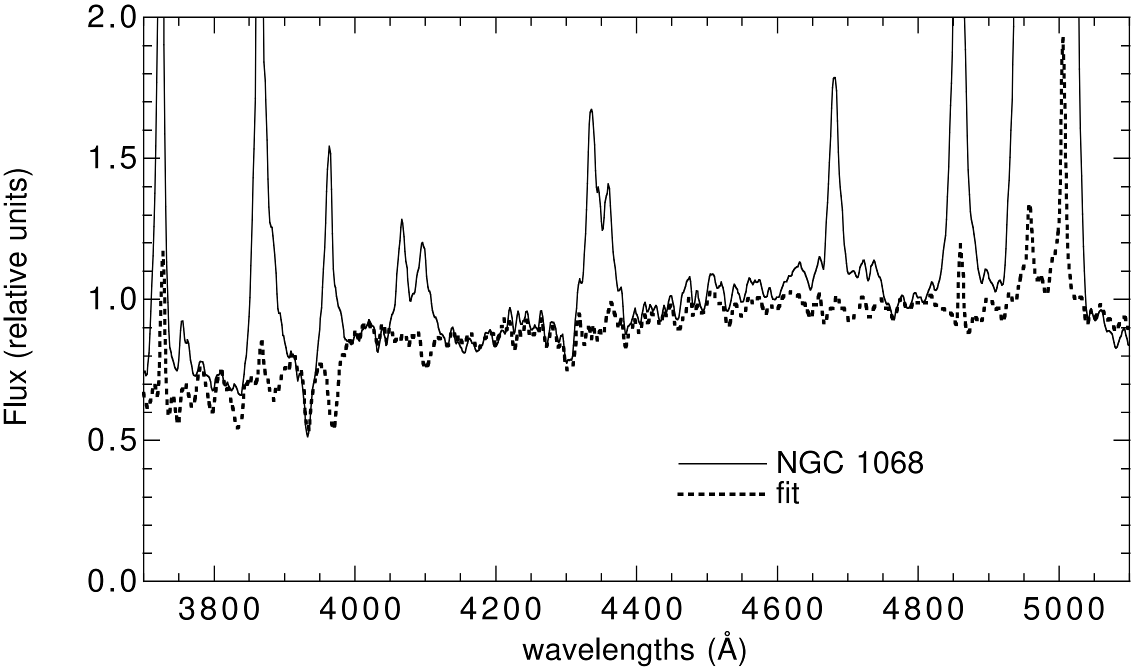

Fig. 12.— Nuclear spectrum of NGC 1068 compared with the result of combining a circumnuclear spectrum (extracted 4 arcsec away from the continuum peak) and a power-law that contributes 10% of the total light at 4800 Å. The nebular continuum contributes 3% to the total light at 4800 Å.

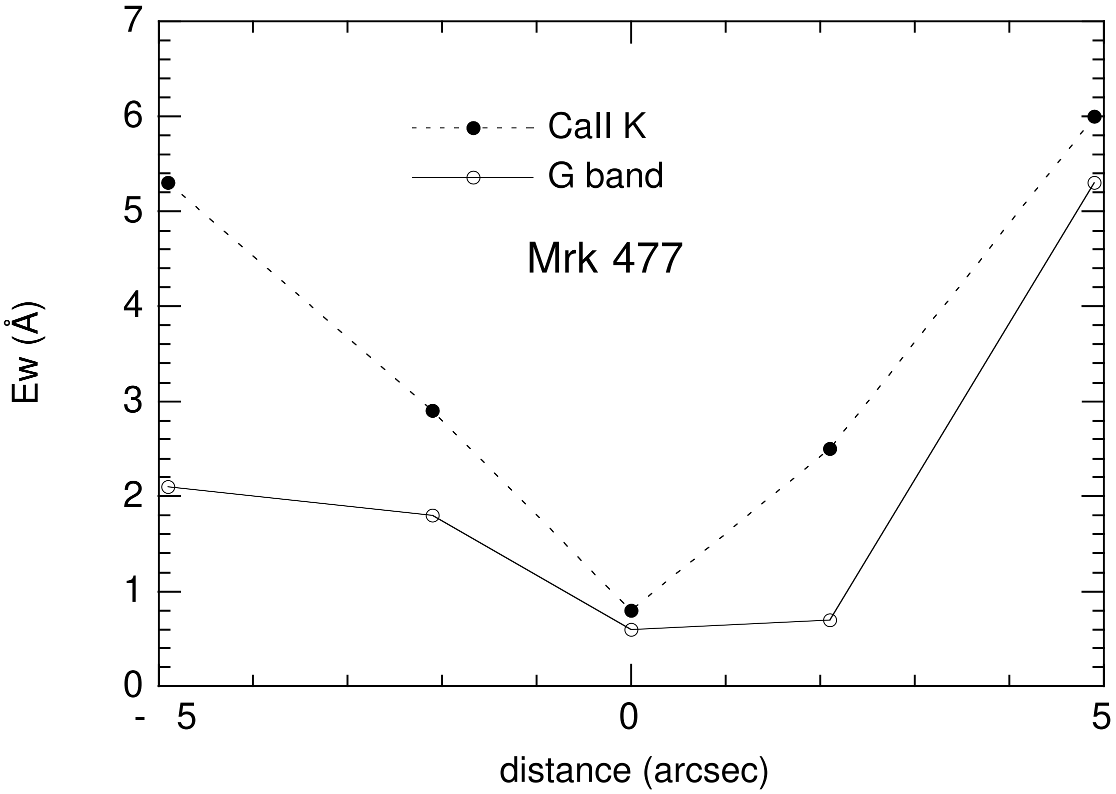

Fig. 13.— Spatial variation of the G band equivalent width (full line) and the CaII K lines (dashed line) toward the nucleus of Mrk 477. Both stellar lines show a significant dilution toward the nucleus.

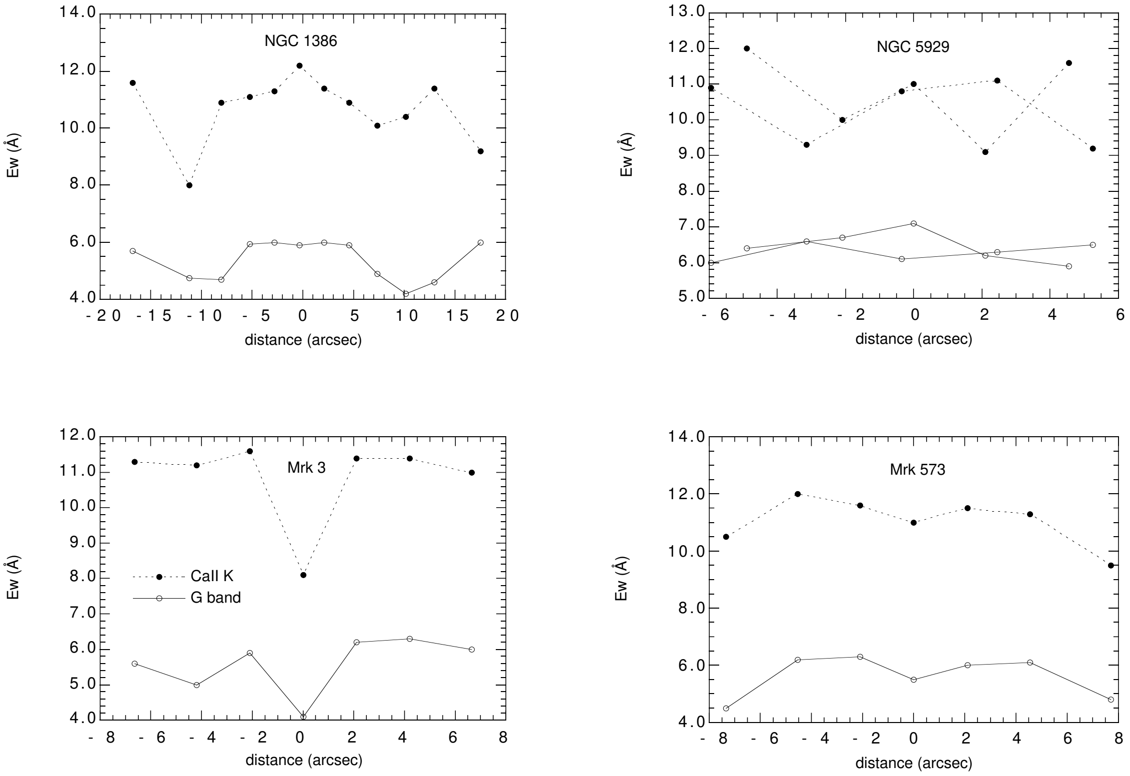

Fig. 14.— As in Figure 13, but for objects with a dominant old stellar population (NGC 1386, NGC 5929, Mrk 573, and Mrk 3). Note that the stellar lines are not significantly diluted in the nuclei of these objects, except in Mrk 3. The two lines (for each stellar feature) in NGC 5929 represent the values measured in two different orientations of the slit.

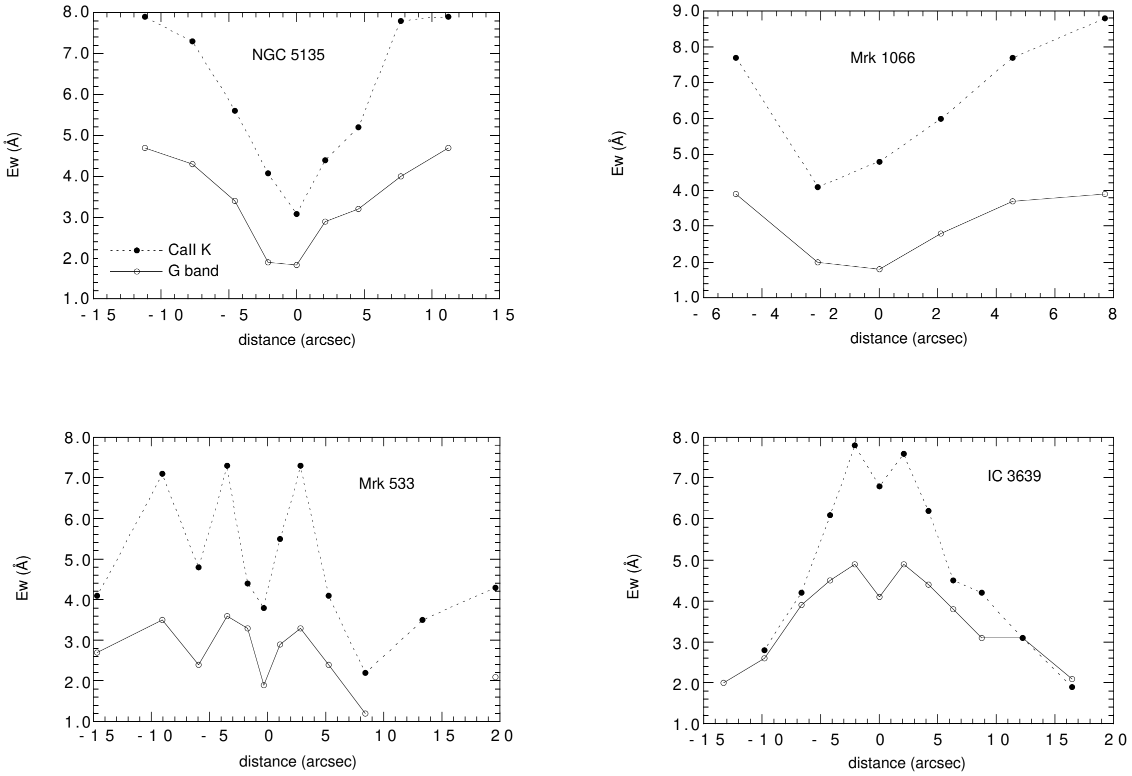

Fig. 15.— As in Figure 13, but for objects that show the higher order terms of the Balmer series in absorption (NGC 5135, Mrk 1066, Mrk 533 and IC 3639). The stellar lines are significantly diluted in the nuclei of these galaxies, probably due to the contribution of a young stellar burst that is more conspicuous in the nucleus.

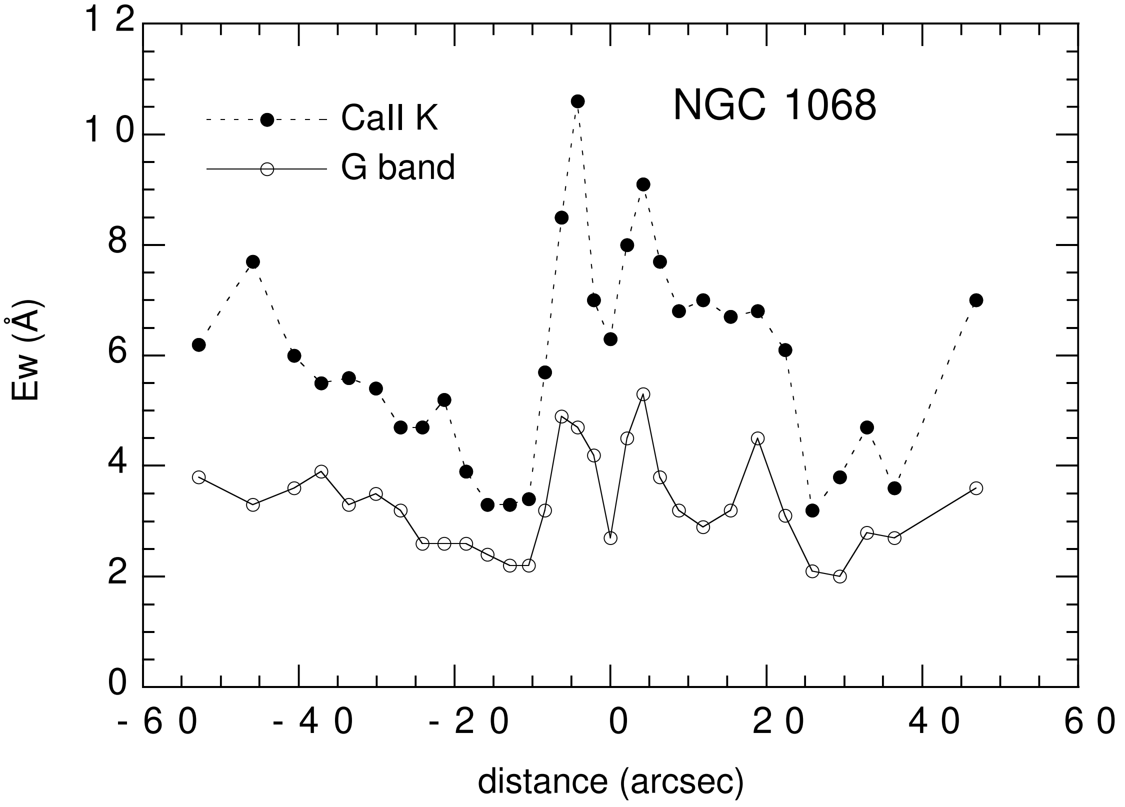

Fig. 16.— As in Figure 13, but for NGC 1068. Note that the decrease of the equivalent width of the stellar lines at ± 10 arcsec away from the continuum peak is due to a change in the stellar population in NGC 1068, produced by the circumnuclear ring of HII regions. The dilution of the stellar lines in the nucleus is associated with the contribution of scattered light from the hidden Seyfert 1 nucleus.

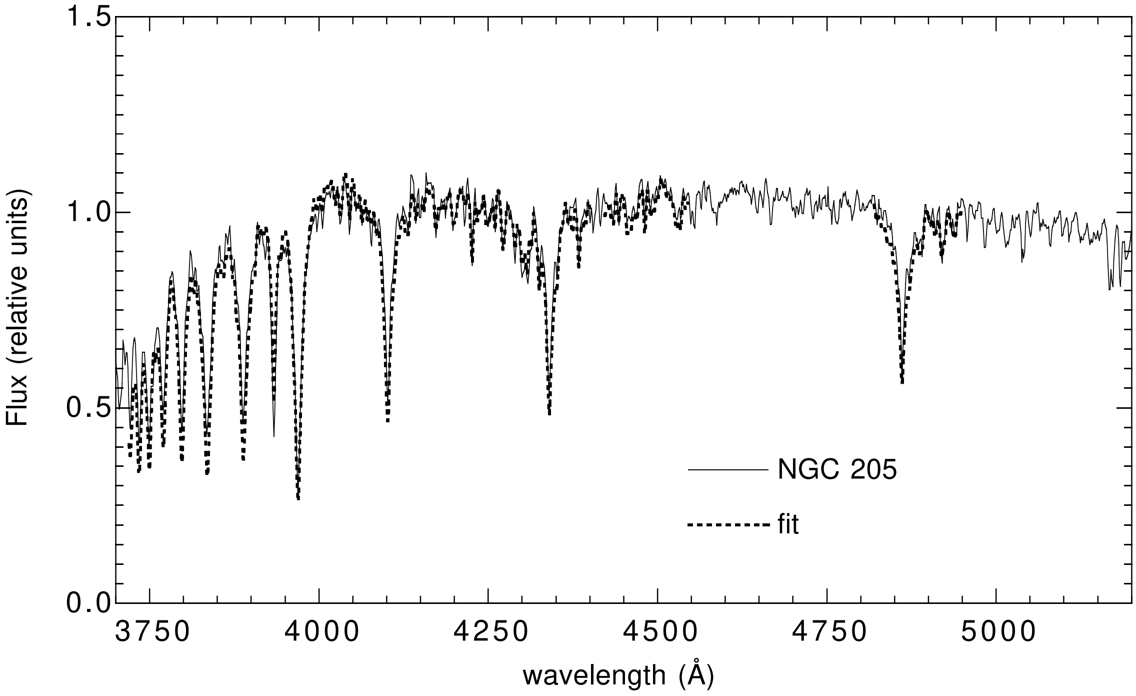

Fig. 17.— Nuclear spectrum of the post-starburst NGC 205 normalized to the flux at 4800 Å, and the best fit (dotted line) obtained by combining the spectrum of the elliptical galaxy NGC 4339 with the average spectrum predicted by our evolutionary models of an intermediate age post-burst (modeled for convenience as a sum of instantaneous bursts of ages 200, 500 and 1000 Myr). The intermediate age population contributes 70% of the total light at 4800 Å. Note that the resulting spectrum fits the stellar lines and the shape of the optical continuum distribution.

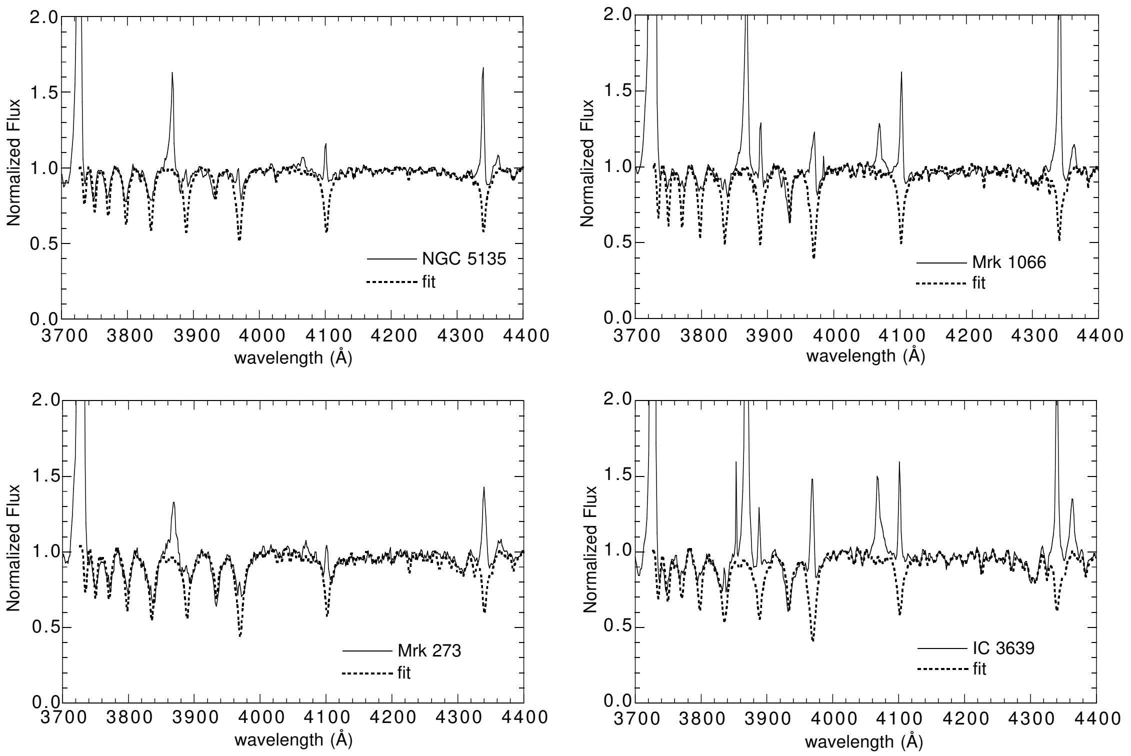

Fig. 18.— Normalized nuclear spectra of NGC 5135 (a), Mrk 1066 (b), Mrk 273 (c), and IC 3639 (d), and the composite model (dotted line) that fits the stellar lines. The best fits are obtained combining the young burst (3 Myr old), an intermediate age population (the average spectrum of three instantaneous bursts of 200, 500 and 1000 Myr old) and an old (10 Gyr) population. The relative contributions to the total light at 4800 Å are: (a) 50%, 40% and 10%; (b) 30%, 50% and 20%; (c) 30%, 40% and 30%; (d) 20%, 40% and 40%, respectively.

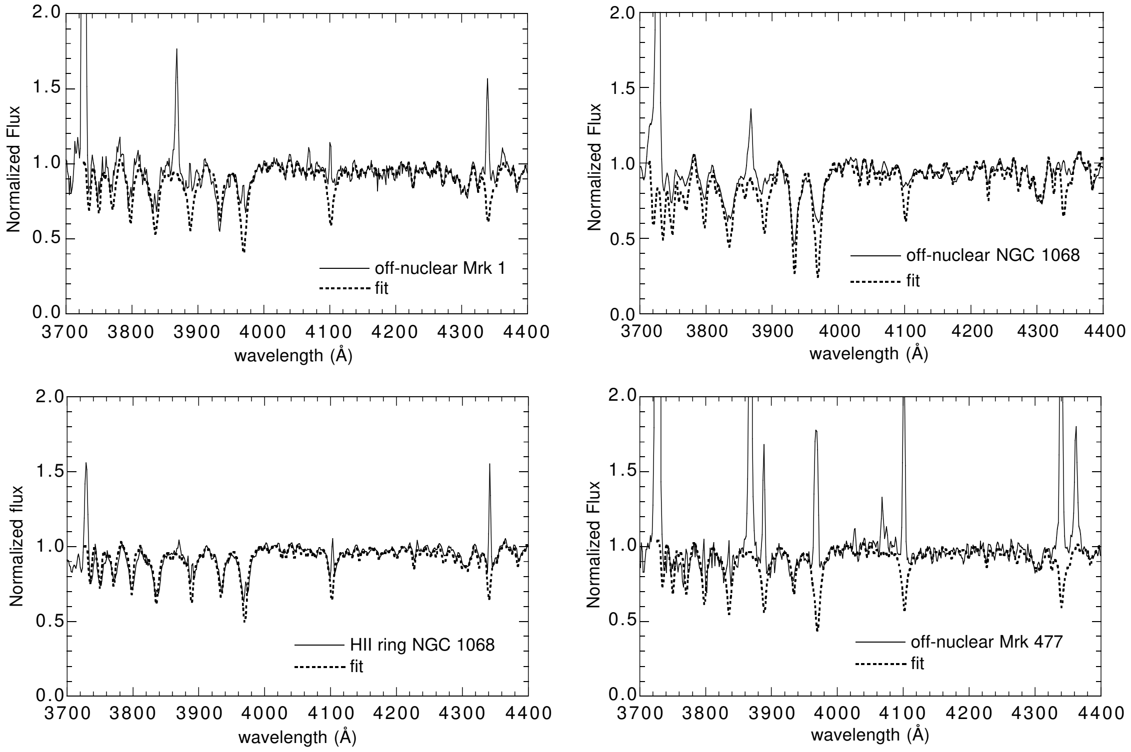

Fig. 19.— As in Figure 17, but for the circumnuclear regions of: (a) Mrk 1 (extracted 3 arcsec from the nucleus); (b) NGC 1068 ("bulge" spectrum extracted 4 arcsec from the continuum peak at 4550 Å); (c) NGC 1068 (HII ring extracted 10 arcsec from the continuum peak); (d) Mrk 477 (extracted 2 arcsec from the nucleus). The best fits are obtained combining a young burst, an intermediate age population, and an old population, except in the "bulge" spectrum of NGC 1068 (which combines an intermediate age and old stellar population). The relative contributions to the total light at 4800 Å are: (a) 20%, 40% and 40%; (c) 40%, 30% and 30%; (d) 30%, 40% and 30%; for the young, intermediate and old stellar population, respectively; and b) 50% and 50% for the intermediate and the old stellar population, respectively.

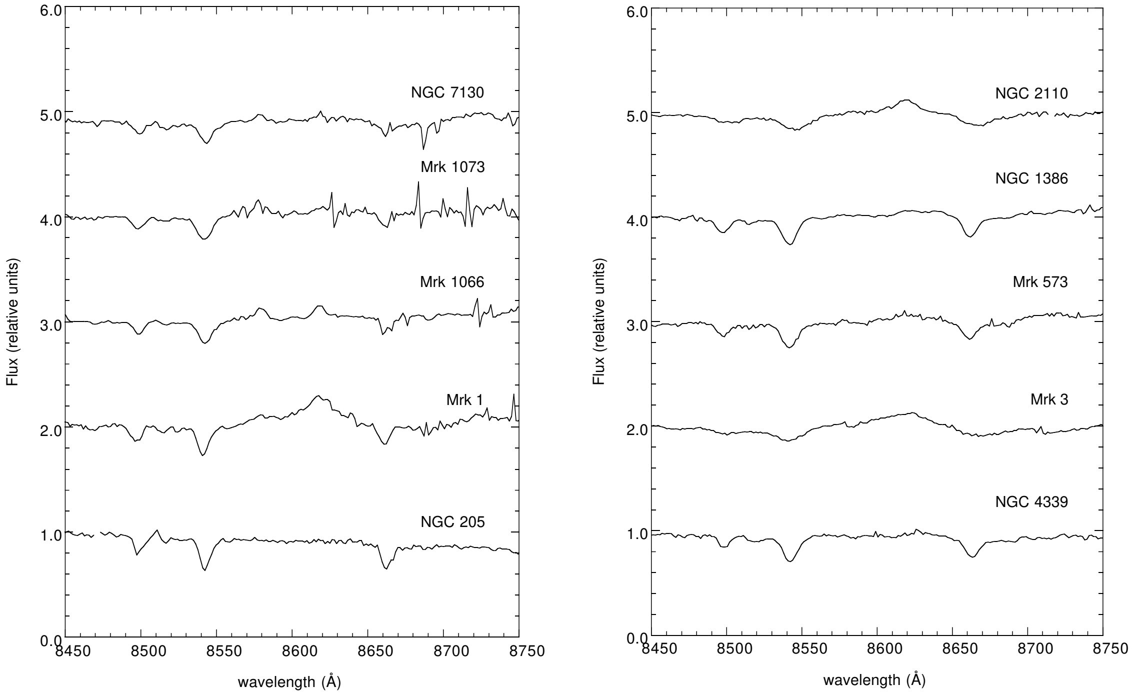

Fig. 20.— Nuclear spectrum in the CaII triplet region normalized to the continuum flux at 8400 Å in (a) objects with a dominant old stellar population: Mrk 3, Mrk 573, NGC 1386 and NGC 2110, and (b) objects that show the higher order terms of the Balmer series in absorption: Mrk 1, Mrk 1066, Mrk 1073 and NGC 7130. The nuclear spectra of the elliptical galaxy NGC 4339 and the post-starburst galaxy NGC 205 are shown for comparison.

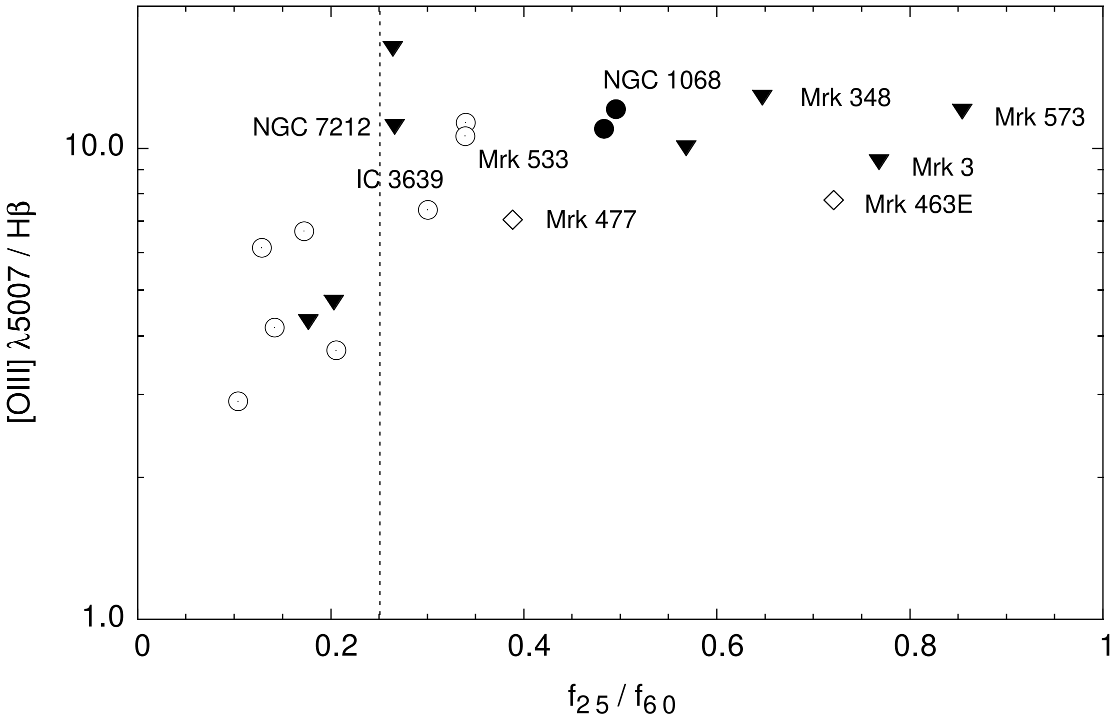

Fig. 21.— Infrared colors $f_{25\mu}/f_{60\mu}$ versus the nuclear excitation ratio [OIII]/Hβ. Symbols are as in Figure 1, and they are marked by the names of the objects.